International Journal of Heat and Mass Transfer 77 (2014) 74–97

Contents lists available at ScienceDirect

International Journal of Heat and Mass Transfer

journal homepage: www.elsevier.com/locate/ijhmt

Review

Review of databases and predictive methods for pressure drop in adiabatic, condensing and boiling mini/micro-channel flows

Sung-Min Kim, Issam Mudawar *

Purdue University Boiling and Two-Phase Flow Laboratory (PU-BTPFL), Mechanical Engineering Building, 585 Purdue Mall, West Lafayette, IN 47907-2088, USA

ARTICLE INFO

Article history:
Received 30 March 2014
Received in revised form 16 April 2014
Accepted 16 April 2014
Available online 4 June 2014

Keywords:
Pressure drop
Flow boiling
Condensation
Mini-channel
Micro-channel

ABSTRACT

Two-phase flow in mini/micro-channels has been the flow configuration of choice for many cooling applications demanding very high rates of heat dissipation per unit volume. Past research aimed at predicting the frictional pressure drop in mini/micro-channels includes a large number of studies that rely on either the Homogeneous Equilibrium Model (HEM) or semi-empirical correlations. But as the number of published studies continues to rise, thermal design engineers are confronted with tremendous confusion when selecting a suitable model or correlation. The primary reason behind this confusion is limited validity of most published methods to a few working fluids and narrow ranges of operating conditions. The present study addresses this limitation by discussing the development of two consolidated mini/micro-channel databases. The first is for adiabatic and condensing flows, and consists of 7115 frictional pressure gradient data points from 36 sources, and the second for boiling flow, and consists of 2378 data points from 16 sources. These consolidated databases are used to assess the accuracy of previous models and correlations as well as to develop 'universal' correlations that are applicable to a large number of fluids and very broad ranges of operating conditions.

Contents

* Corresponding author. Tel.: +1 (765) 494 5705; fax: +1 (765) 494 0539.
E-mail address: mudawar@ecn.purdue.edu (I. Mudawar).
URL: https://engineering.purdue.edu/BTPFL (I. Mudawar).

http://dx.doi.org/10.1016/j.ijheatmasstransfer.2014.04.035
0017-9310/

Nomenclature

Bd	Bond number
Bd^*	modified Bond number
Bo	Boiling number, q''_H/Gh_{fg}
C	parameter in Lockhart–Martinelli [94] correlation
Ca	Capillary number, $Ca = (\mu_f G)/(\rho_f \sigma)$
D	tube diameter
D_h	hydraulic diameter
f	Fanning friction factor
Fr	Froude number
G	mass velocity
g	gravitational acceleration
h	enthalpy
H_{ch}	height of rectangular channel
h_{fg}	latent heat of vaporization
J_f	superficial liquid velocity, $J_f = G(1-x)/\rho_f$
J_g	superficial vapor velocity, $J_g = Gx/\rho_g$
L	length
M	two-phase Mach number
MAE	mean absolute error
N	number of data points
N_{conf}	Confinement number
p	pressure
p_{atm}	atmospheric pressure
p_{crit}	critical pressure
P_F	wetted perimeter of channel
P_H	heated perimeter of channel
P_R	reduced pressure, $P_R = p/p_{crit}$
Δp	pressure drop
q''_{base}	heat flux averaged over base of heat sink
q''_H	effective heat flux averaged over heated perimeter of channel
Re	Reynolds number
Re_{eq}	equivalent Reynolds number
Re_f	superficial liquid Reynolds number, $Re_f = G(1-x)D_h/\mu_f$
Re_{fo}	liquid-only Reynolds number, $Re_{fo} = GD_h/\mu_f$
Re_g	superficial vapor Reynolds number, $Re_g = GxD_h/\mu_g$
Re_{go}	vapor-only Reynolds number, $Re_{go} = GD_h/\mu_g$
Re_{tp}	two-phase Reynolds number, $Re_{tp} = GD_h/\mu_{tp}$
Su	Suratman number
T	temperature
t	time
u	mean velocity
v	specific volume
$\bar{v}$	mixture specific volume
v_{fg}	specific volume difference between saturated vapor and saturated liquid
W	width of heat sink
W_{ch}	width of rectangular channel
We	Weber number
X	Lockhart–Martinelli parameter
x	quality
z	stream-wise coordinate

Greek symbols

α	void fraction
β	channel aspect ratio ($\beta < 1$)
θ	percentage predicted within ±30%
μ	dynamic viscosity
ξ	percentage predicted within ±50%
ρ	density
$\bar{\rho}$	mixture density
σ	surface tension
ϕ	two-phase multiplier; channel inclination angle
Ω	parameter in Chen et al. [103] correlation

Subscripts

A	accelerational
di	dryout incipience
exp	experimental (measured)
F	frictional
f	saturated liquid
fo	liquid only
G	gravitational
g	saturated vapor
go	vapor only
in	channel inlet
k	liquid (f) or vapor (g)
$pred$	predicted
sat	saturation
sub	subcooling
tp	two-phase
tt	turbulent liquid–turbulent vapor
tv	turbulent liquid–laminar vapor
vt	laminar liquid–turbulent vapor
vv	laminar liquid–laminar vapor

1. Introduction

Developers of many modern devices are faced with two conflicting trends: the need to dissipate increasing amounts of heat, and the quest for more compact and lightweight designs. These trends have spurred unprecedented increases in heat dissipation per volume and per surface area, rendering most present air cooling and single-phase liquid cooling solutions virtually obsolete [1,2]. High performance computers, electric vehicle power electronics, avionics, and defense laser and microwave systems are but a few examples of modern applications that are confronted with these trends. Cooling demands in these and many other applications have resulted in a paradigm shift from single-phase to two-phase cooling strategies to capitalize upon the coolant's sensible and latent heat rather the sensible heat alone. And phase change cooling solutions come in a variety of configurations that could meet the system requirements of the application in question. These include pool boiling [3,4], channel flow boiling [5,6], mini/micro-channels [7,8], jet [9–12], spray [13–15], boiling on enhanced surfaces [16–19], and hybrid cooling techniques that combine the benefits of two or more two-phase cooling schemes [20,21].

While most two-phase cooling systems employ air-cooled condensers to reject the heat to the ambient, the quest for more compact and light weight system designs has shifted interest to the use of miniature condensers to reject the heat by condensing a primary coolant in a compact primary cooling loop. The heat is transferred to a secondary liquid coolant and transported to a remote heat exchanger where it is ultimately rejected to the ambient. Employing boiling and condensation in a cooling system has netted orders of magnitude enhancement in heat transfer coefficients and therefore large reductions in cooling system's weight and volume compared to single-phase liquid cooling counterparts.

Among the different two-phase cooling schemes, two-phase flow in mini/micro-channels has been especially favored for its ability to deliver very high heat dissipation per unit area and unit volume, in addition to offering a number of other practical advantages such as ease of fabrication and small coolant inventory. Fig. 1 shows several examples of applications that have benefited greatly

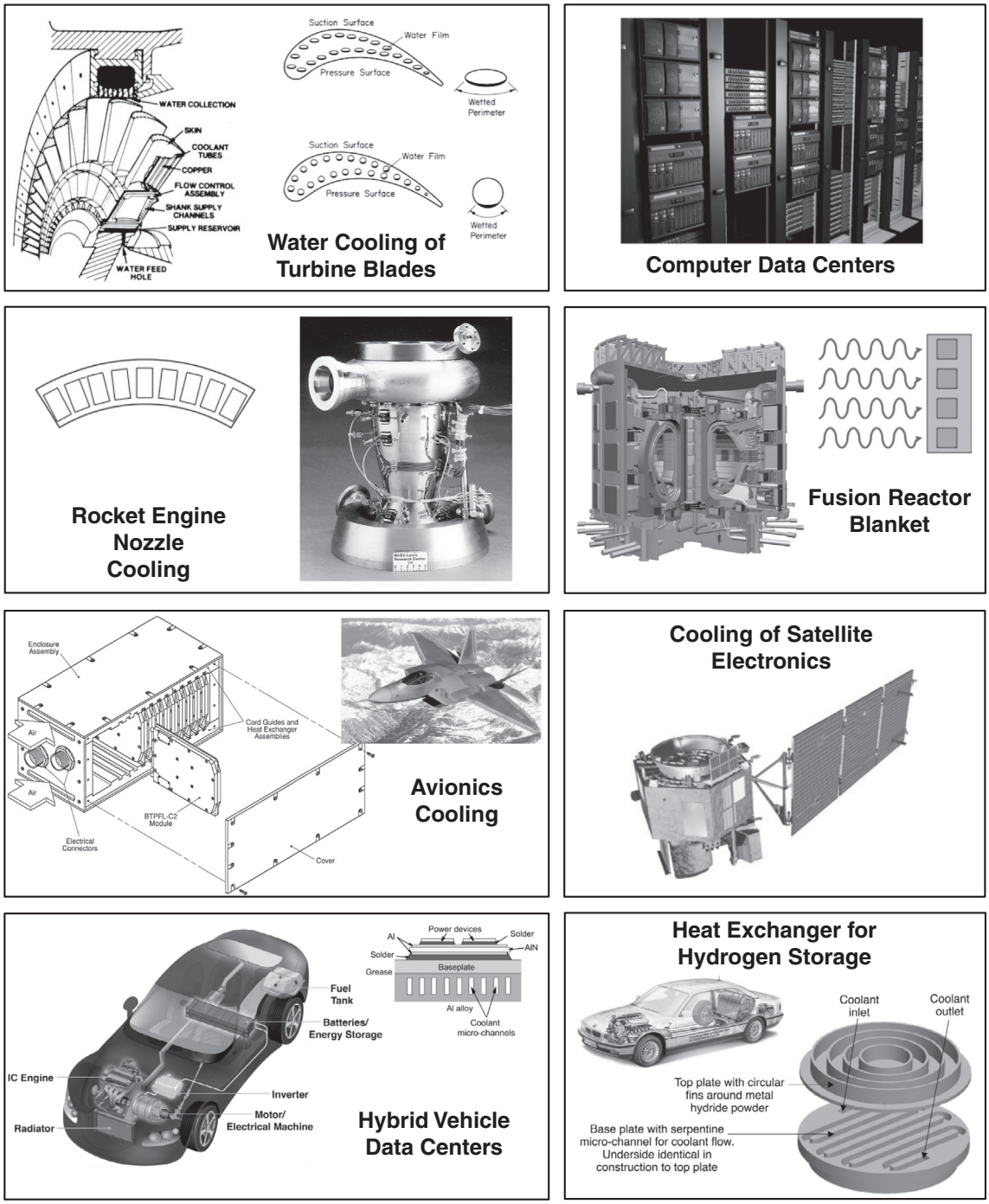

Fig. 1. Examples of applications of high-flux mini/micro-channel cooling.

from two-phase mini/micro-channel flow, including water cooled turbine blades [22], computer data centers [2], rocket nozzle cooling [23], fusion reactor blanket cooling [24,25], avionics cooling [26], cooling of satellite electronics [27], cooling of hybrid vehicle power electronics [28], and heat exchangers for hydrogen storage systems [29]. Fig. 2 illustrates the versatility of mini/micro-channel design, including isolated tubes, tubes that are soldered upon a heat dissipating surface, and channels that are formed into a conducting substrate. There is also great flexibility in mini/micro-channel shape, including circular [30], rectangular [31], triangular [32], trapezoidal [33,34] and diamond [35], with hydraulic diameters in the range of 0.04–2.54 mm.

But two-phase mini/micro-channel devices are not without shortcomings. Key among those is the relatively high pressure drop that accompanies high heat dissipation. And, under certain operating conditions, high pressure drop can result in appreciable compressibility, flashing, or even two-phase choking [30]. Condensation in mini/micro-channels also poses the risk of high pressure drop [36,37]. This highlights the need for reliable predictive tools for pressure drop in two-phase mini/micro-channel flows.

Fig. 3(a) shows schematic representations of the axial variations in pressure and pressure gradient for two-phase condensing flow in a mini/micro-channel with a circumferentially uniform heat flux. The condensation is initiated with formation of a thin liquid

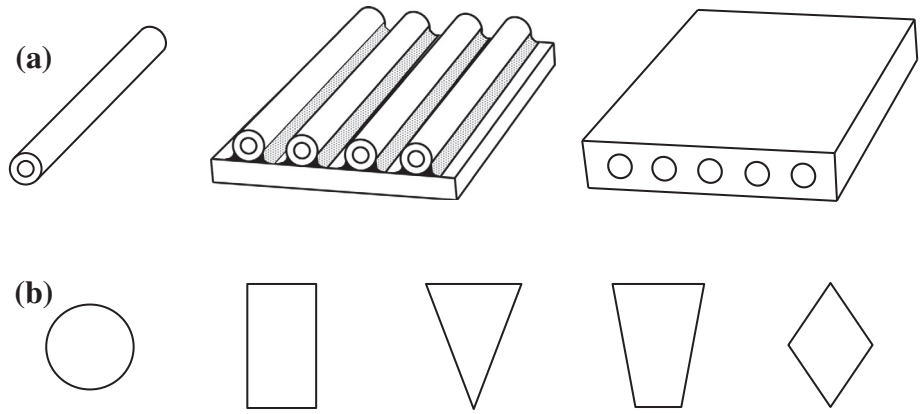

Fig. 2. (a) Implementation of mini/micro-channels in two-phase systems. (b) Examples of mini/micro-channel shapes.

film along the channel walls in the annular flow regime. Increased liquid flow rate is manifest by an axial increase in the film thickness. Large velocity differences between the vapor core and annular liquid film triggers instabilities along the film's interface. Depending on operating conditions, the film flow, which is typically laminar near in the region of film initiation, can turn turbulent. The interfacial waviness increases the interfacial shear stress exerted by the vapor core on the film, thus increasing the pressure gradient. As the film thickens farther downstream, the crests of the large waves begin to merge, bridging liquid films across the channel, and culminating in a transition to the slug flow regime. Further condensation reduces the length of the oblong bubbles, and eventually causes breakup of into smaller bubbles with diameters much smaller than that of the channel in the bubbly flow regime. Ultimately the entire flow is converted to single-phase liquid. Notice that condensation is accompanied by axial deceleration of the flow, and the decreasing velocity difference between the two phases causes a decrease in the interfacial shear stress and a corresponding decrease in the pressure gradient.

Fig. 3(b) shows schematic representations of the axial variations in pressure and pressure gradient for flow boiling along a mini/micro-channel with a circumferentially uniform heat flux. Here, a subcooled liquid entering the channel is heated first at the wall, which causes boiling to be initiated in the wall region, where a bubbly flow regime commences. Further evaporation increases vapor production by increasing both the size and number of bubbles, which increases collision frequency and coalescence between bubbles. In the ensuing slug flow regime, large, oblong bubbles are formed, with a liquid film confined to the wall, and liquid slugs formed between the large bubbles. Further evaporation gradually consumes the liquid slugs, and, in the annular flow regime, the oblong bubbles merge into a continuous vapor core, with a liquid film sheathing the wall. Remnants of the liquid slugs are shattered into droplets that are entrained in the vapor core. The annular regime ceases to exist where the film dries out at the wall. This would occur, of course, only if critical heat flux (CHF) is not encountered upstream. Mist flow, consisting of fine droplets that are dispersed in the vapor flow, is established next. Ultimately, these droplets are fully evaporated as the flow turns into single-phase vapor. Notice that the evaporation causes axial acceleration of the flow, which increases both the wall shear stress and pressure gradient along the channel.

Studies on two-phase flow in mini/micro-channels [31,38–86] have resulted in different approaches to predicting pressure drop. The vast majority of studies concerning two-phase pressure drop prediction are based on the Homogeneous Equilibrium Model (HEM) [87–93] or semi-empirical correlations [42,60,94–109]. But as the number of studies addressing these topics continues to rise, thermal design engineers are confronted with tremendous confusion in selecting a suitable model or correlation. The primary reason behind this confusion is that published predictive methods are limited in validity to specific working fluids and ranges of operating parameters for the data upon which these methods are based. Eliminating this confusion represents an overriding goal of this paper.

The primary objectives of the present study are to:

(1) Provide a comprehensive survey of previous Homogeneous Equilibrium Models and semi-empirical correlations for two-phase frictional pressure drop in both mini/micro-channels and macro-channels.
(2) Review the development of consolidated databases from the world literature for adiabatic, condensing and boiling flows in mini/micro-channels.
(3) Conduct a systematic assessment of previous predictive methods against the consolidated databases.
(4) Discuss the recent development of 'universal' predictive techniques for two-phase frictional pressure drop in adiabatic, condensing and boiling flows in mini/micro-channels, which are based on the consolidated databases.

2. Compressibility, flashing, choking and two-phase flow instabilities

Before addressing predictive tools, it is important to point out some of the anomalies that influence two-phase flow behavior and therefore pressure drop. As mentioned earlier, relatively high pressure drop in micro-channels can result in significant property changes, particularly specific volume and enthalpy of the individual phases. Fig. 4 highlights these effects by comparing pressure drop characteristics for R113 in micro-channel (D_h = 0.51 mm) and mini-channel (D_h = 2.50 mm) heat sinks that are subjected to nearly identical heating conditions. Shown is a relatively mild increase in pressure drop of the mini-channel heat sink, compared to a sharp increase for the micro-channel following the initiation of boiling. As discussed in [30,110], micro-channels can induce sharp increases in pressure drop because of two factors that are the result of property changes: compressibility, which is the result of specific volume variations of vapor and liquid with pressure, and flashing, which is associated with vapor and liquid enthalpy variations with pressure. With high compressibility and flashing comes an increased likelihood of two-phase choking. A simple method to assess these influences is to compare the magnitude of the HEM two-phase Mach number [110]

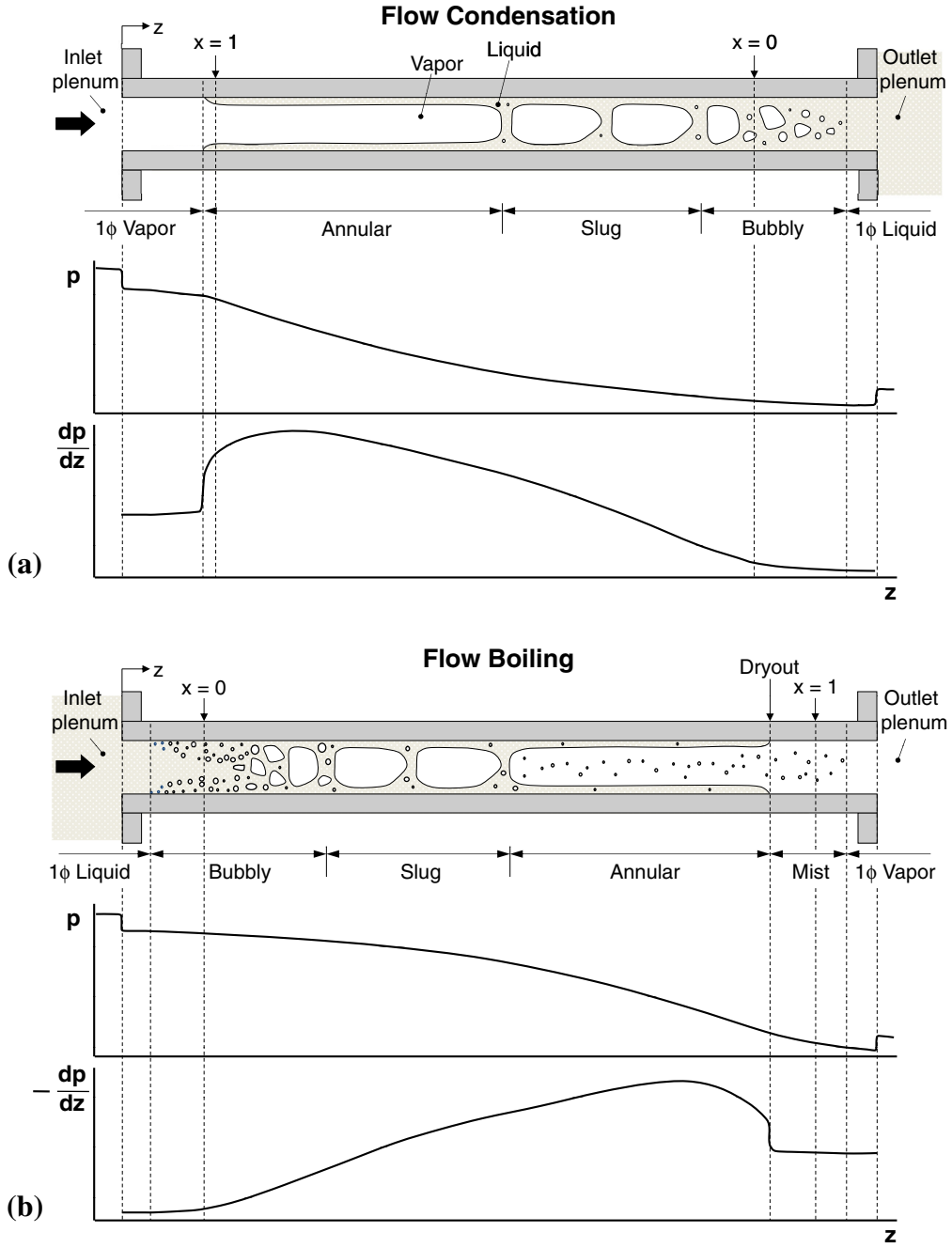

Fig. 3. Schematics of flow regimes and variations of pressure and pressure gradient in mini/micro-channels with uniform circumferential heat flux for (a) flow condensation and (b) flow boiling.

$$M = \left[-G^2 \left\{ x \frac{dv_g}{dp} + (1-x)\frac{dv_f}{dp} \right\} + \frac{G^2 v_{fg}}{h_{fg}} \left\{ x \frac{dh_g}{dp} + (1-x)\frac{dh_f}{dp} \right\} \right]^{1/2} \quad (1)$$

to unity. These effects are considered negligible when $M^2 \ll 1$.

Flow instabilities are a common concern in two-phase systems [111,112]. Small channel size adds further complexity to the identification and prevention of instabilities, especially in mini/micro-channel heat sinks. Instabilities that are unique to these heat sinks are rooted in two-phase compressibility and use of multiple parallel flow channels. Two types of flow instability have been identified in these heat sinks [31]: (1) severe pressure drop oscillation and (2) mild parallel channel instability. The first is the result of communication of the compressible volume in the heat sink with that in the rest of the flow loop. As illustrated in Fig. 5(a), the severe pressure oscillation is manifest by the boiling boundary between the single-phase liquid and two-phase mixture in all channels of the heat sink oscillating back and forth in unison between the inlet and outlet, resulting in a large amplitude pressure oscillation. At high heat fluxes, this instability can escalate further, forcing vapor to flow backwards into the inlet plenum and even induce premature CHF. A common remedy to the severe pressure drop oscillation is to install throttling valves both upstream and downstream of the heat sink in order to dampen the communication of compressibility effects between the heat

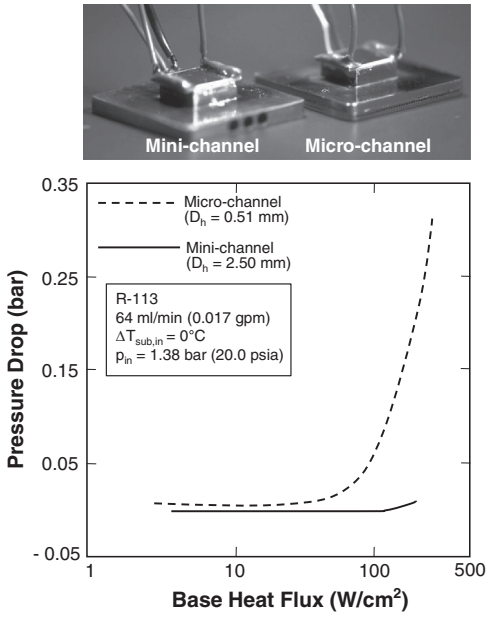

Fig. 4. Comparison of pressure drop characteristics for R113 in micro-channel and mini-channel heat sinks with identical inlet conditions. (Adapted from [110].)

sink and rest of the flow loop. With adequate throttling, only the second mild parallel channel instability is encountered. This instability takes the form of random fluctuations of the boiling boundary between parallel micro-channels as illustrated in Fig. 5(b). Because of the relatively small amplitude of pressure fluctuations, this instability is mild enough to be tolerated during normal cooling system operation.

3. Previous predictive two-phase pressure drop methods

Two-phase pressure drop is generally expressed as the sum of frictional, gravitational and accelerational (or decelerational) components,

$$\Delta P_{tp} = \Delta P_{tp,F} + \Delta P_{tp,G} + \Delta P_{tp,A}. \tag{2}$$

$\Delta P_{tp,A}$ is positive for boiling flows because of flow acceleration along the stream-wise direction, negative for condensing flows because of flow deceleration, and negligible for adiabatic flows. The accelerational pressure gradient can be expressed as

$$-\left(\frac{dP}{dz}\right)_A = G^2 \frac{d}{dz}\left[\frac{\upsilon_g x^2}{\alpha} + \frac{\upsilon_f (1-x)^2}{(1-\alpha)}\right]. \tag{3}$$

The gravitational pressure gradient is expressed as

$$-\left(\frac{dp}{dz}\right)_G = [\alpha\rho_g + (1-\alpha)\rho_f] g \sin\phi, \tag{4}$$

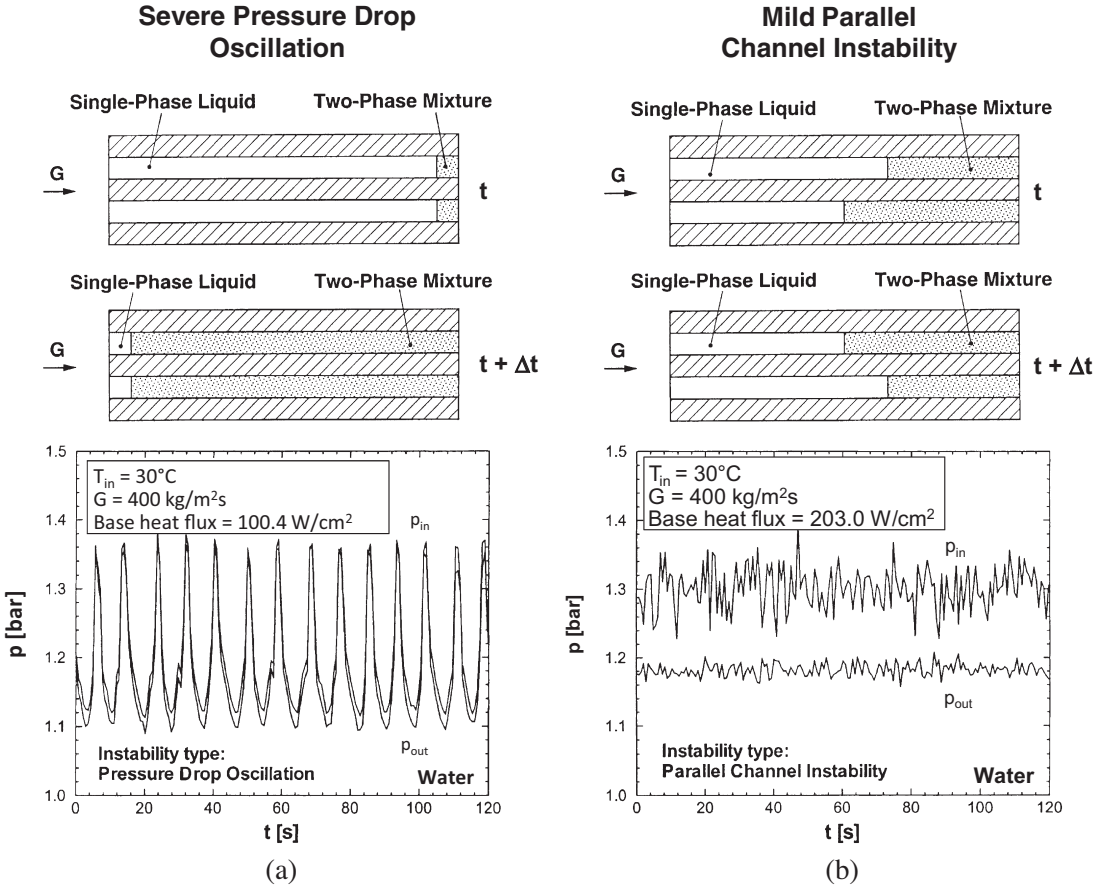

Fig. 5. Top view depictions of two neighboring micro-channels, and temporal records of inlet and outlet pressures during (a) severe pressure drop oscillation and (b) mild parallel channel instability. (Adapted from [31].)

where ϕ is the channel's inclination angle; $-\left(\frac{dp}{dz}\right)_G = 0$ for horizontal flow. Unlike macro-channel flows, where gravitational effects can be significant, especially for low mass velocities, these effects are far less significant for mini/micro-channel flows, which are dominated by high velocities and large shear stresses.

A popular method to relating the void fraction, α, to flow quality, x, is to use Zivi's relation [113],

$$\alpha = \left[1 + \left(\frac{1-x}{x}\right)\left(\frac{\rho_g}{\rho_f}\right)^{2/3}\right]^{-1}. \tag{5}$$

An alternative to using Zivi's relation to determine the accelerational and gravitational pressure gradients is to use the HEM, which provides a simple relation between mixture density and mixture specific volume,

$$\alpha\rho_g + (1-\alpha)\rho_f = \bar{\rho} = \frac{1}{\bar{v}} = \frac{1}{x v_g + (1-x)v_f}, \tag{6}$$

which yields

$$\alpha = \left[1 + \left(\frac{1-x}{x}\right)\left(\frac{v_f}{v_g}\right)\right]^{-1}, \tag{7}$$

where x is set equal to the thermodynamic equilibrium quality in the saturation region of the channel. Eq. (7) can be used to reduce the accelerational and gravitational pressure gradients, given by Eqs. (3) and (4), respectively, to

$$-\left(\frac{dp}{dz}\right)_A = G^2\frac{d\left[x v_g + (1-x)v_f\right]}{dz} \tag{8}$$

and

$$-\left(\frac{dp}{dz}\right)_G = \frac{g\sin\phi}{x v_g + (1-x)v_f}. \tag{9}$$

The two-phase frictional pressure drop, $\Delta P_{tp,F}$, can be predicted according to either the HEM or semi-empirical correlations. Using the HEM, the two-phase frictional pressure gradient can be determined from [114]

$$-\left(\frac{dP}{dz}\right)_F = \frac{2f_{tp}\bar{\rho}u^2}{D_h} = \frac{2f_{tp}v_f G^2}{D_h}\left(1 + x\frac{v_{fg}}{v_f}\right), \tag{10}$$

where

$$f_{tp} = 16\ Re_{tp}^{-1} \text{ for } Re_{tp} < 2000, \tag{11a}$$

$$f_{tp} = 0.079\ Re_{tp}^{-0.25} \text{ for } 2000 \leqslant Re_{tp} < 20,000 \tag{11b}$$

and

$$f_{tp} = 0.046\ Re_{tp}^{-0.2} \text{ for } Re_{tp} \geqslant 20,000. \tag{11c}$$

Table 1
Two-phase mixture viscosity models employed in the Homogeneous Equilibrium Model (HEM).

Author(s)	Equation
McAdams et al. [87]	$\frac{1}{\mu_{tp}} = \frac{x}{\mu_g} + \frac{1-x}{\mu_f}$
Akers et al. [88]	$\mu_{tp} = \frac{\mu_f}{\left[(1-x)+x\left(\frac{v_g}{v_f}\right)^{0.5}\right]}$
Cicchitti et al. [89]	$\mu_{tp} = x\mu_g + (1-x)\mu_f$
Owens [90]	$\mu_{tp} = \mu_f$
Dukler et al. [91]	$\mu_{tp} = \frac{xv_g\mu_g + (1-x)v_f\mu_f}{xv_g + (1-x)v_f}$
Beattie and Whalley [92]	$\mu_{tp} = \omega\mu_g + (1-\omega)(1+2.5\omega)\mu_f$ $\omega = \frac{xv_g}{v_f + xv_{fg}}$
Lin et al. [93]	$\mu_{tp} = \frac{\mu_f\mu_g}{\mu_g + x^{1.4}(\mu_f - \mu_g)}$

Different predictions of $\Delta P_{tp,F}$ are possible, depending on which mixture viscosity model is used to calculate the two-phase Reynolds number, Re_{tp} (=GD_h/μ_{tp}). Table 1 provides a summary of the most popular two-phase mixture viscosity models.

Table 2 provides a summary of two-phase frictional pressure gradient correlations that have been recommended previously for macro-channels [94–98] and mini/micro-channels [42,60,99–109] for adiabatic, condensing, and boiling flows. Most of these correlations are based on the Lockhart–Martinelli separated flow model [94], with the two-phase frictional pressure gradient expressed as the product of the frictional pressure gradient for each phase (based on actual flow rate for the individual phase) and a corresponding two-phase pressure drop multiplier.

$$\left(\frac{dP}{dz}\right)_F = \left(\frac{dP}{dz}\right)_f \phi_f^2 = \left(\frac{dP}{dz}\right)_g \phi_g^2, \tag{12}$$

where

$$-\left(\frac{dP}{dz}\right)_f = \frac{2f_f v_f G^2(1-x)^2}{D_h} \tag{13a}$$

and

$$-\left(\frac{dP}{dz}\right)_g = \frac{2f_g v_g G^2 x^2}{D_h}. \tag{13b}$$

Relations for the two-phase pressure drop multipliers are available in terms of the Lockhart–Martinelli parameter, X, and are dependent on the liquid and vapor flow states. The friction factor for phase k (which denotes f for liquid or g for vapor) in Eqs. (13a) and (13b) is given by

$$f_k = 16\,Re_k^{-1} \text{ for } Re_k < 2000, \tag{14a}$$

$$f_k = 0.079\,Re_k^{-0.25} \text{ for } 2000 \leqslant Re_k < 20,000 \tag{14b}$$

and

$$f_k = 0.046\,Re_k^{-0.2} \text{ for } Re_k \geqslant 20,000, \tag{14c}$$

where

$$Re_k = Re_f = \frac{G(1-x)D_h}{\mu_f} \text{ for liquid} \tag{15a}$$

and

$$Re_k = Re_g = \frac{G_x D_h}{\mu_g} \text{ for vapor.} \tag{15b}$$

For laminar flow in rectangular channels, the two-phase friction factor can be expressed in terms of the channel's aspect ratio [115],

$$f_k Re_k = 24\left(1 - 1.3553\beta + 1.9467\beta^2 - 1.7012\beta^3 + 0.9564\beta^4 - 0.2537\beta^5\right). \tag{16}$$

The correlations in Table 2 are used to determine the two-phase frictional pressure gradient. The two-phase pressure drop can be determined by integrating the relations for accelerational, gravitational and frictional pressure gradients numerically according to

$$\Delta P_{tp} = \int_0^{L_{tp}} \left[-\left(\frac{dP}{dz}\right)_F - \left(\frac{dP}{dz}\right)_G - \left(\frac{dP}{dz}\right)_A\right] dz. \tag{17}$$

As indicated earlier, use of a particular frictional pressure gradient correlation must conform to the specific fluids and ranges of operating conditions of the database the correlation is based upon as indicated in Table 2. To determine the two-phase frictional pressure drop in macro-channels, the correlations of Friedel [95] and Müller-Steinhagen and Heck [96] are recommended because of their reliance on very large databases, 25,000 and 9300 data points, respectively. Based on adiabatic air–water flow in 1–4 mm diame-

Table 2
Two-phase frictional pressure gradient correlations.

Author(s)	Equation	Remarks
Recommended for macro-channels		
Lockhart and Martinelli [94]	$\left(\frac{dp}{dz}\right)_F = \left(\frac{dp}{dz}\right)_f \phi_f^2, \phi_f^2 = 1 + \frac{C}{X} + \frac{1}{X^2}, X^2 = \frac{(dp/dz)_f}{(dp/dz)_g}$ $C_{vv} = 5, C_{tv} = 10, C_{vt} = 12, C_{tt} = 20$	D_h = 1.49–25.83 mm, adiabatic, water, oils, hydrocarbons
Friedel [95]	$\left(\frac{dp}{dz}\right)_F = \left(\frac{dp}{dz}\right)_{fo} \phi_{fo}^2$ $\phi_{fo}^2 = (1-x)^2 + x^2\left(\frac{v_g}{v_f}\right)\left(\frac{f_{go}}{f_{fo}}\right) + 3.24x^{0.78}(1-x)^{0.224}\left(\frac{v_g}{v_f}\right)^{0.91}\left(\frac{\mu_g}{\mu_f}\right)^{0.19}\left(1-\frac{\mu_g}{\mu_f}\right)^{0.7}$ $Fr_{tp}^{-0.045} We_{tp}^{-0.035}$ $Fr_{tp} = \frac{G^2}{gD_h\rho_H^2}, \quad We_{tp} = \frac{G^2 D_h}{\sigma\rho_H}, \rho_H = \frac{1}{xv_g + (1-x)v_f}$	D > 4 mm, air–water, air-oil, R12 (25,000 data points)
Müller-Steinhagen and Heck [96]	$\left(\frac{dp}{dz}\right)_F = \left\{\left(\frac{dp}{dz}\right)_{fo} + 2\left[\left(\frac{dp}{dz}\right)_{go} - \left(\frac{dp}{dz}\right)_{fo}\right]x\right\}(1-x)^{1/3} + \left(\frac{dp}{dz}\right)_{go} x^3$	D = 4–392 mm, air–water, water, hydrocarbons, refrigerants (9300 data points)
Jung and Radermacher [97]	$\left(\frac{dp}{dz}\right)_F = \left(\frac{dp}{dz}\right)_{fo} \phi_{fo}^2, \phi_{fo}^2 = 12.82 X_{tt}^{-1.47}(1-x)^{1.8}$ $X_{tt} = \left(\frac{\mu_f}{\mu_g}\right)^{0.1}\left(\frac{1-x}{x}\right)^{0.9}\left(\frac{\rho_g}{\rho_f}\right)^{0.5}$	D = 9.1 mm, annular flow boiling, pure and mixed refrigerants
Wang et al. [98]	For $G \geqslant 200$ kg/m^2s: $\left(\frac{dp}{dz}\right)_F = \left(\frac{dp}{dz}\right)_g \phi_g^2, \phi_g^2 = 1 + 9.4X^{0.62} + 0.564X^{2.45}$ For $G < 200$ kg/m^2s: $\left(\frac{dp}{dz}\right)_F = \left(\frac{dp}{dz}\right)_f \phi_f^2, \phi_f^2 = 1 + \frac{C}{X} + \frac{1}{X^2},$ $C = 4.566 \times 10^{-6} X^{0.128} Re_{fo}^{0.938}\left(\frac{v_f}{v_g}\right)^{2.15}\left(\frac{\mu_f}{\mu_g}\right)^{5.1}$	D = 6.5 mm, adiabatic, R22, R134a, R407C
Recommended for mini/micro-channels		
Mishima and Hibiki [99]	$\left(\frac{dp}{dz}\right)_F = \left(\frac{dp}{dz}\right)_f \phi_f^2, \phi_f^2 = 1 + \frac{C}{X} + \frac{1}{X^2}$ For rectangular channels: $C = 21[1 - exp(-0.319D_h)]$; D_h [mm] For circular tubes: $C = 21[1 - exp(-0.333D)]$; D [mm]	D = 1.05–4.08 mm, adiabatic, air–water
Yang and Webb [42]	$\left(\frac{dp}{dz}\right)_F = -0.87 Re_{eq}^{0.12} f_{fo} \frac{G_{eq}^2 v_f}{D_h}, \quad Re_{eq} = \frac{G_{eq} D_h}{\mu_f}$ $G_{eq} = G\left[(1-x) + x\left(\frac{\rho_f}{\rho_g}\right)^{0.5}\right]$	D_h = 1.56, 2.64 mm, adiabatic, R12, $Re_{fo} > 2500$
Yan and Lin [100]	$\left(\frac{dp}{dz}\right)_F = -0.22 Re_{eq}^{-0.1} \frac{G_{eq}^2 v_f}{D_h}$	D = 2.0 mm, boiling, R134a, Re_{eq} > 1000
Yan and Lin [101]	$\left(\frac{dp}{dz}\right)_F = -996.6 Re_{eq}^{-1.074} \frac{G_{eq}^2 v_f}{D_h}$	D = 2.0 mm, condensation, R134a, Re_{eq} > 2000
Tran et al. [102]	$\left(\frac{dp}{dz}\right)_F = \left(\frac{dp}{dz}\right)_{fo} \phi_{fo}^2, \quad N_{conf} = \sqrt{\frac{\sigma}{g(\rho_f - \rho_g)D_h^2}}\left(= \sqrt{\frac{1}{Bd}}\right)$ $\phi_{fo}^2 = 1 + \left[4.3\frac{(dp/dz)_{go}}{(dp/dz)_{fo}} - 1\right]\left[N_{conf} x^{0..875}(1-x)^{0.875} + x^{1.75}\right]$	D_h = 2.40–2.92 mm, boiling, refrigerants
Chen et al. [103]	$\left(\frac{dp}{dz}\right)_F = \left(\frac{dp}{dz}\right)_{fo.Friedel} \Omega, \quad Bd^* = g\left(\rho_f - \rho_g\right)\frac{(D_h/2)^2}{\sigma}$ For $Bd^* < 2.5 : \Omega = \frac{0.0333 Re_{fo}^{0.45}}{Re_g^{0.09}(1+0.4e^{-Bd^*})}$ For $Bd* \geqslant 2.5 : \Omega = \frac{We_{tp}^{0.2}}{(2.5+0.06Bd^*)}$	D = 1.02–9 mm, adiabatic, air–water, R410A, ammonia
Lee and Lee [104]	$\left(\frac{dp}{dz}\right)_F = \left(\frac{dp}{dz}\right)_f \phi_f^2, \quad \phi_f^2 = 1 + \frac{C}{X} + \frac{1}{X^2}, \quad \psi = \frac{\mu_f J_f}{\sigma}, \quad \lambda = \frac{\mu_f^2}{\rho_f \sigma D_h}$ $C_{vv} = 6.833 \times 10^{-8} \lambda^{-1.317} \psi^{0.719} Re_{fo}^{0.557}, \quad C_{tv} = 3.627 Re_{fo}^{0.174}$ $C_{vt} = 6.185 \times 10^{-2} Re_{fo}^{0.726}, \quad C_{tt} = 0.048 Re_{fo}^{0.451}$	D_h = 0.78–6.67 mm, adiabatic, air–water
Yu et al. [105]	$\left(\frac{dp}{dz}\right)_F = \left(\frac{dp}{dz}\right)_f \phi_f^2, \quad \phi_f^2 = \left[18.65\left(\frac{v_f}{v_g}\right)^{0.5}\left(\frac{1-x}{x}\right)\frac{Re_g^{0.1}}{Re_f^{0.5}}\right]^{-1.9}$	D = 2.98 mm, boiling, water, Re_f < 2000 and Re_g > 2000
Hwang and Kim [60]	$\left(\frac{dp}{dz}\right)_F = \left(\frac{dp}{dz}\right)_f \phi_f^2, \quad \phi_f^2 = 1 + \frac{C}{X} + \frac{1}{X^2}, \quad C = 0.227 Re_{fo}^{0.452} X^{-0.32} N_{conf}^{-0.82}$	D = 0.244, 0.430, 0.792 mm, adiabatic, R134a, Re_{fo} < 2000
Sun and Mishima [106]	For Re_f < 2000 and Re_g < 2000: $\left(\frac{dp}{dz}\right)_F = \left(\frac{dp}{dz}\right)_f \phi_f^2, \quad \phi_f^2 = 1 + \frac{C}{X} + \frac{1}{X^2}, \quad C = 26\left(1 + \frac{Re_f}{1000}\right)\left[1 - \exp\left(\frac{-0.153}{0.27N_{conf}^2 + 0.8}\right)\right]$ For $Re_f \geqslant 2000$ or $Re_g \geqslant 2000$: $\left(\frac{dp}{dz}\right)_F = \left(\frac{dp}{dz}\right)_f \phi_f^2, \quad \phi_f^2 = 1 + \frac{C}{X^{1.19}} + \frac{1}{X^2}, \quad C = 1.79\left(\frac{Re_g}{Re_f}\right)^{0.4}\left(\frac{1-x}{x}\right)^{0.5}$	D_h = 0.506–12 mm, air–water, refrigerants, CO_2 (2092 data points)
Li and Wu [107]	$\left(\frac{dp}{dz}\right)_F = \left(\frac{dp}{dz}\right)_f \phi_f^2, \quad \phi_f^2 = 1 + \frac{C}{X} + \frac{1}{X^2}, \quad Bd = \frac{g(\rho_f - \rho_g)D_h^2}{\sigma}$ For $Bd \leqslant 1.5$: $C = 11.9 Bd^{0.45}$ For $1.5 < Bd \leqslant 11$: $C = 109.4\left(BdRe_f^{0.5}\right)^{-0.56}$ For $Bd > 11$: Beattie and Whalley [92] correlation is recommended	D_h = 0.148–3.25 mm, adiabatic, refrigerants, ammonia, propane, nitrogen (769 data points)
Zhang et al. [108]	$\left(\frac{dp}{dz}\right)_F = \left(\frac{dp}{dz}\right)_f \phi_f^2, \quad \phi_f^2 = 1 + \frac{C}{X} + \frac{1}{X^2}$ For adiabatic liquid–gas flow: $C = 21[1 - \exp(-0.674/N_{conf})]$ For adiabatic liquid–vapor flow: $C = 21[1 - \exp(-0.142/N_{conf})]$	D_h = 0.07–6.25 mm, adiabatic, air/N_2–water, air/ethanol, refrigerants, ammonia, water (2201 data points), not recommended for turbulent liquid–turbulent vapor (tt) flow

(*continued on next page*)

Table 2 (*continued*)

Author(s)	Equation	Remarks
Li and Wu [109]	For $Bd < 0.1$: $\left(\frac{dp}{dz}\right)_F = \left(\frac{dp}{dz}\right)_f \phi_f^2, \quad \phi_f^2 = 1 + \frac{C}{X} + \frac{1}{X^2}, \quad C = 5.60Bd^{0.28}$ For $Bd \geqslant 0.1$ and $BdRe_f^{0.5} \leqslant 200$: $\left(\frac{dp}{dz}\right)_F = \left(\frac{dp}{dz}\right)_{fo} \phi_{fo}^2, \quad \phi_{fo}^2 = (1-x)^2 + 2.87x^2P_R^{-1} + 1.54Bd^{0.19}\left(\frac{\rho_f - \rho_g}{\rho_H}\right)^{0.81}$ For $BdRe_f^{0.5} > 200$: Beattie and Whalley [92] correlation is recommended	Same data as Li and Wu [107]

ter circular tubes, Mishima and Hibiki's correlation [99] has yielded good predictions of mini/micro-channel pressure drop data for both adiabatic flow [54,62] and flow boiling [31,79]. Other correlations with relatively broad geometrical and flow parameters include those of Sun and Mishima [106], Li and Wu [107,109], and Zhang et al. [108], with 2092, 769 and 2201 mini/micro-channel pressure drop data points, respectively.

Use of a particular correlation must also conform to the laminar or turbulent flow states for the individual phases for certain correlations. For example, the correlations of Yang and Webb [42] and Yan and Lin [101], which are based on an equivalent Reynolds number Re_{eq} proposed by Akers et al. [88], are valid only for turbulent flows ($Re_{fo} > 2500$ for [42], and $Re_{eq} > 2000$ for [101]). The correlation of Yu et al. [105] is recommended for laminar liquid-turbulent vapor flow ($Re_f < 2000$ and $Re_g > 2000$). On the other hand, Hwang and Kim's [60] correlation is based on data corresponding to $Re_{fo} < 2000$, and the correlation of Zhang et al. [108], a modified form of Mishima and Hibiki's [99], is not recommended for turbulent liquid-turbulent vapor flows.

4. Pressure drop in adiabatic and condensing flows

4.1. Consolidation of world databases for adiabatic and condensing mini/micro-channel flows

Despite the abundance of correlations to predict pressure drop in mini/micro-channel flows, the vast majority of these correlations are suitable to a relatively small number of working fluids, let alone limited ranges of key geometrical and flow parameters. To derive a 'universal' correlation, it is crucial to amass a database that encompasses the largest number of working fluids and broadest ranges of all operating parameters. Acquiring such databases has been a primary objective for a series of studies that have been recently conducted at the Purdue University Boiling and Two-Phase Flow Laboratory (PU-BTPFL). These studies involved systematic consolidation of world databases for mini/micro-channels, and development of universal predictive tools for pressure drop [116,117], heat transfer coefficient [118,119], and dryout incipience quality [120], following a methodology that was devised earlier to predict flow boiling CHF for water flow in tubes [25,121,122].

A total of 7115 frictional pressure drop data points for both adiabatic and condensing flows in mini/micro-channels were amassed from 36 sources [38–73]. The database includes 2387 adiabatic gas–liquid data points from 10 sources, 3531 adiabatic liquid–vapor data points from 20 sources, and 1197 condensation data points from 8 sources. Table 3 describes the individual databases comprising the consolidated database. An important attribute of the new consolidated database is its broad range of reduced pressure, from 0.0052 to 0.91.

It is important to note that all the condensation data included in Table 3 correspond to relatively small quality decrements, Δx. Therefore, by assuming a linear quality variation along the channel, an average of the inlet and outlet qualities is used in the development of a pressure drop correlation. Additionally, because of the small quality decrement, the contribution of the deceleration term to total pressure drop is found to be quite small for most of the data. The frictional pressure drop component in the 1197 condensation data points was determined by the original authors by subtracting the accelerational and gravitational pressure drop components from the measured total pressure drop. To calculate the decelerational pressure drop, Coleman [45], Mitra [57], Andresen [58] and Marak [68] used a void fraction relation by Baroczy [123], while Rouhani and Axelsson's [124] used a relation by Huang et al. [70]. The Baroczy, and Rouhani and Axelsson void fraction relations are given, respectively, by

$$\alpha = \left[1 + \left(\frac{1-x}{x}\right)^{0.74}\left(\frac{\rho_g}{\rho_f}\right)^{0.65}\left(\frac{\mu_f}{\mu_g}\right)^{0.13}\right]^{-1} \tag{18}$$

and

$$\alpha = \frac{x}{\rho_g}\left[\{1 + 0.12(1-x)\}\left(\frac{x}{\rho_g} + \frac{1-x}{\rho_f}\right) + \frac{1.18(1-x)\left\{g\sigma\left(\rho_f - \rho_f\right)\right\}^{0.25}}{G\rho_f^{0.5}}\right]^{-1}. \tag{19}$$

4.2. Assessment of previous frictional pressure gradient correlations against consolidated database for adiabatic and condensing mini/micro-channel flows

The consolidated database for adiabatic and condensing mini/micro-channel flows is used to assess the accuracy of previous HEMs and semi-empirical correlations in predicting the two-phase frictional pressure gradient, using Eqs. (10) and (12), respectively. Thermophysical properties for different fluids are evaluated using NIST's REFPROP 8.0 software [125], excepting those for FC-72, which are obtained from 3M Company. Three different parameters are used to assess the accuracy of individual models or correlations. θ and ξ are defined as the percentages of data points predicted within ±30% and ±50%, respectively, and MAE the mean absolute error, which is determined according to

$$MAE = \frac{1}{N}\sum \frac{\left|dP/dz_{F,pred} - dP/dz_{F,exp}\right|}{dP/dz_{F,exp}} \times 100\%. \tag{20}$$

Predictions of previous HEMs [87–93], semi-empirical correlations for macro-channels [94–98], and semi-empirical correlations for mini/micro-channels [42,60,99–109] are compared to three subsets of the 7115 point consolidated database: adiabatic liquid–gas flow, adiabatic liquid–vapor flow, and condensing flow, as shown in Table 4. Most of the viscosity models used in conjunction with the HEM show poor predictions of the adiabatic liquid–gas data. The viscosity model of Dukler et al. [91] and correlation of Mishima and Hibiki [99] generally provide good predictions for adiabatic liquid–gas flow, with MAE values of 33.7% and 34.1%, respectively. For adiabatic liquid–vapor flow, the correlation of Müller-Steinhagen and Heck [96] shows the best accuracy, with

Table 3
Two-phase frictional pressure drop data for adiabatic and condensing mini/micro-channel flows included in the consolidated database [116].

Author(s)	Channel geometry[a]	Channel material		Fluid(s)	G [kg/m^2 s]	Test mode	Data points
Hinde et al. [38]	C single, H	Copper	4.57	R134a, R12	149–298	Condensation Δx = 0.1–0.35	45
Wambsganss et al. [39]	R single, H	Plexiglas	5.44	Air–water	50–500	Adiabatic	112
Fujita et al. [40]	R single, H	Acrylic, nickel	0.39, 2.14, 3.33	N_2–water, N_2–ethanol	32–815	Adiabatic	167
Hirofumi and Webb [41]	C/R multi, H	Aluminum	0.96–2.13	R134a	194–1404	Adiabatic	58
Yang and Webb [42]	R multi, H	Aluminum	2.64	R12, R134a	400–1400	Adiabatic	64
Triplett et al. [43]	C/semi triangular single, H	Pyrex glass, acrylic	1.088, 1.097, 1.447	Air–water	23–6010	Adiabatic	192
Bao et al. [44]	C single, H	Copper	1.95	Air–water	110–435	Adiabatic	135
Coleman [45]	C single/multi, R multi, H	Aluminum	0.761–4.910	R134a	150–750	Adiabatic	245
Coleman [45]	C/R multi, H	Aluminum	0.424–1.524	R134a	150–750	Condensation Δx = 0.05–0.1	261
Wang et al. [46]	C single, H	Copper	3.0	R410A, R407C, R22	400	Adiabatic	45
Zhang and Webb [47]	C single/multi, H	Copper, Aluminum	2.13, 3.25, 6.20	R134a, R22, R404A	400–1000	Adiabatic	72
Nino et al. [48]	R multi, H	Aluminum	1.02, 1.54	R410A, R134a	50–300	Adiabatic	364
Nino et al. [48]	R multi, H	Aluminum	1.02, 1.54	Air–water	55–220	Adiabatic	121
Adams et al. [49]	R multi, H	Aluminum	1.02, 1.54	CO_2, ammonia, R245fa	50–440	Adiabatic	245
Monroe et al. [50]	R multi, H	Aluminum	1.66	R134a	49–402	Adiabatic	32
Pehlivan [51]	C single, H	Glass	0.8, 1.0, 3.0	Air–water	236–2252	Adiabatic	130
Jang and Hrnjak [52]	C single, H	Copper	6.10	CO_2	198–406	Adiabatic	54
Shin [53]	C/R single, H	Copper	0.493–1.067	R134a	100–600	Condensation small Δx	247
Tu and Hrnjak [54]	R single, H	PVC	0.0695–0.3047	R134a	102–785	Adiabatic	264
Cavallini et al. [55]	R multi, H	Aluminum	1.4	R410A, R134a, R236ea	200–1400	Adiabatic	51
Chen et al. [56]	C single, H	Copper	3.25	R410A	300–600	Adiabatic	26
Mitra [57]	C single, H	Copper	6.22	R410A	400–800	Condensation Δx = 0.21 (avg)	118
Andresen [58]	C single/multi, H	Aluminum, copper	0.76, 1.52, 3.05	R410A	200–800	Condensation Δx = 0.32 (avg)	291
English and Kandlikar [59]	R single, H	Lexan	1.018	air–water	4–32	Adiabatic	40
Hwang and Kim [60]	C single, H	Stainless steel	0.244, 0.430, 0.792	R134a	140–950	Adiabatic	77
Yun et al. [61]	R multi, H	Stainless steel	1.437	R410A	200–400	Adiabatic	19
Field and Hrnjak [62]	R single, H	Aluminum	0.148	R134a, R410A, propane, ammonia	290–590	Adiabatic	67
Park and Hrnjak [63]	C single/multi, H	Aluminum, copper	0.89, 3.5, 6.1	CO_2, R410A, R22	100–600	Adiabatic	146
Revellin and Thome [64]	C single, H	Glass	0.517	R134a, R245fa	309–1926	Adiabatic	1331
Yue et al. [65]	R single, H	PMMA	0.667	CO_2-water	91–1020	Adiabatic	105
Quan et al. [66]	trapezoidal multi, H	Silicon wafer, glass cover	0.109, 0.142, 0.151	Water	90–288	Condensation small Δx	65
Dutkowski [67]	C single, H	Stainless steel	0.64–2.30	Air–water	139–8528	Adiabatic	465
Marak [68]	C single, VU	Stainless steel	1.0	Methane	162–701	Condensation Δx = 0.04 (avg)	135
Park and Hrnjak [69]	C multi, H	Aluminum	0.89	CO_2	200–800	Adiabatic	52
Huang et al. [70]	C single, H	Copper	1.6, 4.18	R410A	200–600	Condensation Δx = 0.2	35
Choi et al. [71]	R single, H	Glass	0.143, 0.322, 0.490	N_2-water	65–1080	Adiabatic	920
Ducoulombier et al. [72]	C single, H	Stainless steel	0.529	CO_2	200–1400	Adiabatic	292
Tibiriçá and Ribatski [73]	C single, H	Stainless steel	2.32	R245fa	100–500	Adiabatic	27
Total							7115

[a] C: circular, R: rectangular, H: horizontal, VU: vertical upflow.

Table 4
Assessment of universal correlation for adiabatic and condensing mini/micro-channel flows and previous models and correlations with two-phase frictional pressure gradient databases for adiabatic liquid–gas flow, adiabatic liquid–vapor flow, and condensing flow [116,117]. Bracketed values indicate number of data points used for evaluation.

Author(s)	Adiabatic liquid–gas (2387 data points)			Adiabatic liquid–vapor (3531 data points)			Condensation (1197 data points)			Boiling (2378 data points)		
	MAE (%)	θ (%)	ξ (%)	MAE (%)	θ (%)	ξ (%)	MAE (%)	θ (%)	ξ (%)	MAE (%)	θ (%)	ξ (%)
McAdams et al. [87]	75.0	44.8	61.7	35.2	35.8	83.2	38.4	32.3	87.6	52.3	12.7	51.9
Akers et al. [88]	130.5	37.4	49.6	32.4	50.9	89.6	27.2	57.9	95.2	40.6	29.4	75.7
Cicchitti et al. [89]	412.1	27.9	38.7	41.1	59.0	85.8	65.0	60.0	92.1	56.5	40.0	83.3
Owens [90]	571.3	25.9	36.8	71.6	59.2	76.3	98.1	66.6	87.9	55.4	55.0	83.9
Dukler et al. [91]	33.7	48.6	77.8	38.1	29.6	73.7	35.9	31.0	86.2	48.2	12.9	48.0
Beattie and Whalley [92]	36.1	58.2	78.5	33.2	43.7	88.9	27.6	53.0	94.2	41.8	22.3	66.1
Lin et al. [93]	150.4	35.9	50.5	34.1	40.7	88.2	40.2	38.8	89.4	56.8	17.5	61.6
Lockhart and Martinelli [94]	47.1	44.2	70.9	83.6	32.1	42.7	142.9	17.0	26.1	41.6	58.2	72.7
Friedel [95]	422.9	14.7	24.5	62.2	60.3	76.0	56.7	72.3	85.6	47.6	65.6	86.0
Müller-Steinhagen and Heck [96]	39.3	50.6	73.9	26.0	68.8	90.1	23.6	79.2	93.7	31.2	52.9	87.6
Jung and Radermacher [97]	314.3	11.6	20.7	137.1	24.0	39.1	169.4	12.1	20.6	53.6	46.1	67.8
Wang et al. [98]	63.1	32.7	55.8	59.1	40.2	58.9	83.5	19.4	33.2	35.7	52.4	72.1
Mishima and Hibiki [99]	34.1	54.9	85.0	41.5	41.8	65.3	58.3	46.8	65.4	27.6	61.3	91.6
Yang and Webb [42]	40.3 [398]	37.2 [398]	59.5 [398]	34.6 [1781]	43.1 [1781]	76.4 [1781]	23.6 [789]	68.9 [789]	89.7 [789]	39.1 [1489]	30.7 [1489]	69.9 [1489]
Yan and Lin [100]	155.0 [960]	29.1 [960]	39.2 [960]	189.9 [3332]	4.4 [3332]	9.0 [3332]	265.5 [1170]	0.3 [1170]	0.8 [1170]	120.9 [2349]	14.7 [2349]	25.1 [2349]
Yan and Lin [101]	247.9 [752]	19.8 [752]	27.7 [752]	173.3 [3056]	15.2 [3056]	26.3 [3056]	142.2 [1070]	20.9 [1070]	35.0 [1070]	94.7 [2261]	29.1 [2261]	46.7 [2261]
Tran et al. [102]	1179.9	1.5	3.4	280.0	6.2	9.9	438.5	11.7	20.3	296.3	27.1	41.9
Chen et al. [103]	39.2	38.7	66.3	55.7	13.7	33.4	52.0	24.1	45.4	48.1	24.7	42.3
Lee and Lee [104]	44.9	33.8	56.5	86.6	29.4	44.6	258.9	13.6	20.7	55.3	41.9	62.3
Yu et al. [105]	74.2 [391]	1.8 [391]	13.8 [391]	70.4 [1891]	1.4 [1891]	12.2 [1891]	69.7 [459]	0.2 [459]	9.2 [459]	73.8 [1300]	1.5 [1300]	6.7 [1300]
Hwang and Kim [60]	44.0 [1917]	31.4 [1917]	53.1 [1917]	37.4 [1541]	52.8 [1541]	71.3 [1541]	27.1 [333]	69.1 [333]	88.3 [333]	44.5 [692]	42.2 [692]	74.7 [692]
Sun and Mishima [106]	37.5	42.3	75.1	34.1	59.8	86.4	20.1	80.5	97.7	32.3	42.1	86.4
Li and Wu [107]	37.0	48.5	82.0	38.8	55.0	79.0	36.0	50.5	78.3	35.9	41.9	73.5
Zhang et al. [108]	35.2 [2230]	52.6 [2230]	80.8 [2230]	39.7 [2252]	36.1 [2252]	67.0 [2252]	33.1 [552]	42.2 [552]	87.0 [552]	43.3 [1806]	19.3 [1806]	65.1 [1806]
Li and Wu [109]	205.7	38.2	60.1	49.5	52.2	74.4	33.9	56.1	82.5	34.1	45.8	75.7
Universal correlation	25.7	67.5	92.3	23.7	70.8	93.7	17.5	85.0	99.2	17.2	85.9	97.4

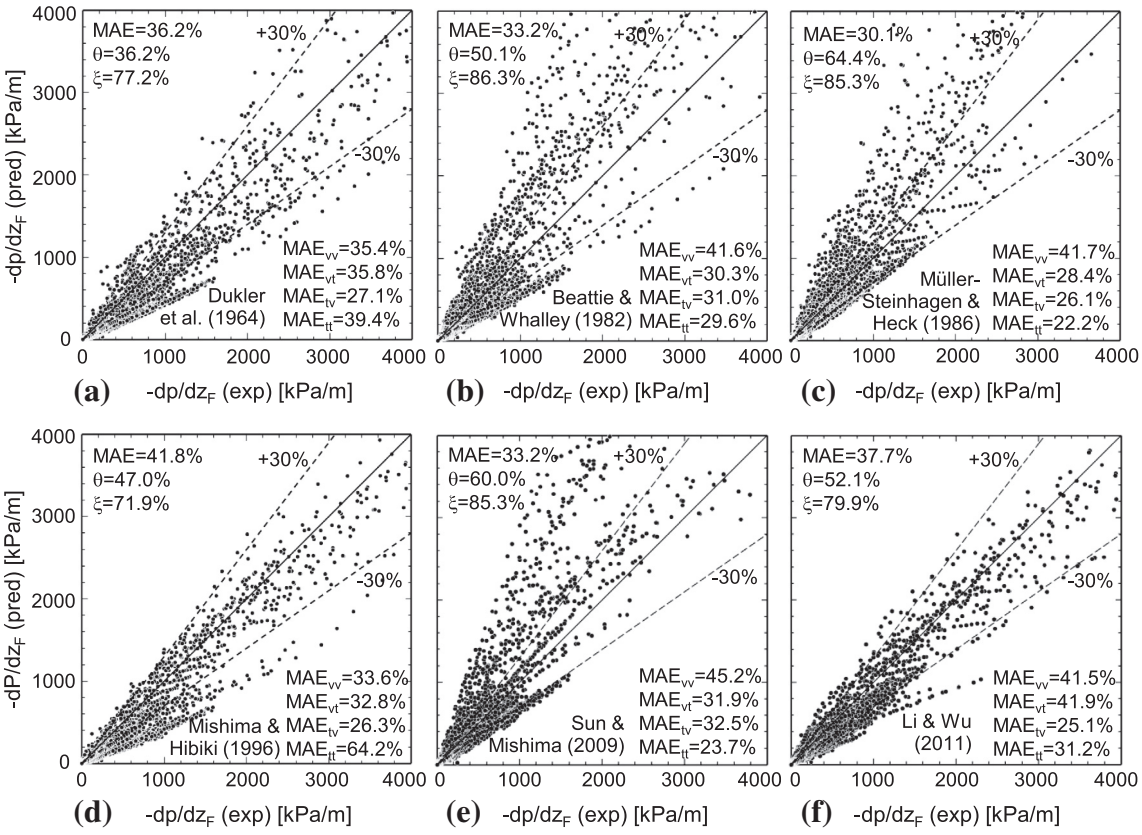

Fig. 6. Comparison of 7115 point consolidated database for frictional pressure gradient for adiabatic and condensing mini/micro-channel flows with predictions of HEM using mixture viscosity models of (a) Dukler et al. [91] and (b) Beattie and Whalley [92], and semi-empirical correlations of (c) MÜller-Steinhagen and Heck [96], (d) Mishima and Hibiki [99], (e) Sun and Mishima [106], and (f) Li and Wu [107]. (Adapted from [116].)

a MAE of 26.0%. And for condensing flow, best predictions are achieved with the correlations of Müller-Steinhagen and Heck and Sun and Mishima [106], with MAE values of 23.6%, and 20.1%, respectively. However, the predictive capabilities of these models and correlations are compromised for specific subsets of the consolidated database, such as Müller-Steinhagen and Heck and Sun and Mishima for adiabatic liquid–gas data, and Dukler et al. and Mishima and Hibiki for adiabatic liquid–vapor and condensation data.

Fig. 6 compares the 7115 point consolidated mini/micro-channel database with predictions of select HEMs as well as semi-empirical correlations that have shown relatively superior predictive capability. The MAEs for laminar liquid-laminar vapor (*vv*), laminar liquid-turbulent vapor (*vt*), turbulent liquid-laminar vapor (*tv*), and turbulent liquid-turbulent vapor laminar (*tt*) flow regimes are indicated as MAE_{vv}, MAE_{vt}, MAE_{tv} and MAE_{tt}, respectively. Fig. 6 shows the model of Dukler et al. [91] generally underpredicts the consolidated database. Among the semi-empirical correlations, those of Müller-Steinhagen and Heck [96] and Sun and Mishima [106] show less favorable predictions in the *vv* regime, and Mishima and Hibiki's [99] in the *tt* regime.

4.3. Universal predictive method based on consolidated database for adiabatic and condensing mini/micro-channel flows

A universal approach to predicting two-phase frictional pressure drop for adiabatic and condensing mini/micro-channel flows was developed by replacing the constant *C* in the original formulation of Lockhart and Martinelli [94] with a function of dimensionless groups that capture the influences of small channel size, different working fluids, and broad ranges of flow parameters. Table 5 provides a summary of new *C* functions of liquid-only Reynolds number, Re_{fo}, vapor-only (or gas-only) Suratman number, Su_{go}, and density ratio, ρ_f/ρ_g, for each of the four flow regimes (*tt*, *tv*, *vt*, and *vv*) that yield the least MAE versus the consolidated database. Fig. 7 shows the universal two-phase frictional pressure drop correlation predicts the entire 7115 experimental mini/micro-channel database quite accurately, with MAE values of 26.3%, 22.4%, 26.8%, and 21.1% for the *vv*, *vt*, *tv* and *tt* flow regimes, respectively.

To further examine the predictive accuracy of the universal correlation, individual mini/micro-channel databases from 36 sources are compared in Table 6 with predictions of the universal correlation as well as select previous models and correlations that have shown relatively superior predictive capability. The models by Dukler et al. [91] and Beattie and Whalley [92] show good predictions of some of the data for adiabatic liquid–gas flow, such as those of Nino et al. [48], English and Kandlikar [59] and Dutkowski [67]. The correlations of Müller-Steinhagen and Heck [96] and Sun and Mishima [106] provide good predictions for most of the adiabatic liquid–vapor and condensation databases, respectively. Overall, the universal correlation provides excellent predictive capability against all individual databases, with 19 databases predicted more accurately than with any of the select previous models or correlations, and the best overall MAE of 23.3%, with 72.1% and 94.1% of the data falling within ±30% and ±50% error bands, respectively.

Predictions of the universal correlation and Müller-Steinhagen and Heck [96] correlation are compared with representative adiabatic flow data [47,49] and condensation data [45,58] in Fig. 8(a), (b) and (c), (d), respectively. The frictional pressure gradient increases with increasing mass velocity in both the experimental data and predictions. The correlation of Müller-Steinhagen and

Table 5
Universal two-phase frictional pressure drop correlation for adiabatic and condensing mini/micro-channel flows in both single- and multi-channel configurations [116].

$\left(\frac{dp}{dz}\right)_F = \left(\frac{dp}{dz}\right)_f \phi_f^2$

where $\phi_f^2 = 1 + \frac{C}{X} + \frac{1}{X^2}$, $X^2 = \frac{(dp/dz)_f}{(dp/dz)_g}$

$-\left(\frac{dp}{dz}\right)_f = \frac{2f_f v_f G^2 (1-x)^2}{D_h}$, $-\left(\frac{dp}{dz}\right)_g = \frac{2f_g v_g G^2 x^2}{D_h}$

$f_k = 16 Re_k^{-1}$ for $Re_k < 2000$

$f_k = 0.079 Re_k^{-0.25}$ for $2000 \leqslant Re_k < 20{,}000$

$f_k = 0.046 Re_k^{-0.2}$ for $Re_k \geqslant 20{,}000$

for laminar flow in rectangular channel:

$f_k Re_k = 24\left(1 - 1.3553\beta + 1.9467\beta^2 - 1.7012\beta^3 + 0.9564\beta^4 - 0.2537\beta^5\right)$

where subscript k denotes f or g for liquid and vapor phases, respectively,

$Re_f = \frac{G(1-x)D_h}{\mu_f}$, $Re_g = \frac{GxD_h}{\mu_g}$, $Re_{fo} = \frac{GD_h}{\mu_f}$, $Su_{go} = \frac{\rho_g \sigma D_h}{\mu_g^2}$

	C
$Re_f \geqslant 2000$, $Re_g \geqslant 2000$ (tt)	$0.39 Re_{fo}^{0.03} Su_{go}^{0.10} \left(\frac{\rho_f}{\rho_g}\right)^{0.35}$
$Re_f \geqslant 2000$, $Re_g < 2000$ (tv)	$8.7 \times 10^{-4} Re_{fo}^{0.17} Su_{go}^{0.50} \left(\frac{\rho_f}{\rho_g}\right)^{0.14}$
$Re_f < 2000$, $Re_g \geqslant 2000$ (vt)	$0.0015 Re_{fo}^{0.59} Su_{go}^{0.19} \left(\frac{\rho_f}{\rho_g}\right)^{0.36}$
$Re_f < 2000$, $Re_g < 2000$ (vv)	$3.5 \times 10^{-5} Re_{fo}^{0.44} Su_{go}^{0.50} \left(\frac{\rho_f}{\rho_g}\right)^{0.48}$

Correlation based on consolidated database of 7115 frictional pressure drop data points from 36 sources with the following application range:
- Working fluids: air/CO_2/N_2–water mixtures, N_2–ethanol mixture, R12, R22, R134a, R236ea, R245fa, R404A, R410A, R407C, propane, methane, ammonia, CO_2, and water
- Hydraulic diameter: 0.0695 $< D_h <$ 6.22 mm
- Mass velocity: 4.0 $< G <$ 8528 kg/m^2 s
- Liquid-only Reynolds number: 3.9 $< \mathrm{Re}_{fo} = GD_h/\mu_f <$ 89,798
- Superficial liquid Reynolds number: 0 $< \mathrm{Re}_f = G(1-x)D_h/\mu_f <$ 79,202
- Superficial vapor (or gas) Reynolds number: 0 $< Re_g = G\,x\,D_h/\mu_g <$ 253,810
- Flow quality: 0 $< x <$ 1
- Reduced pressure (for 4728 condensing and adiabatic liquid–vapor data): 0.0052 $< P_R <$ 0.91

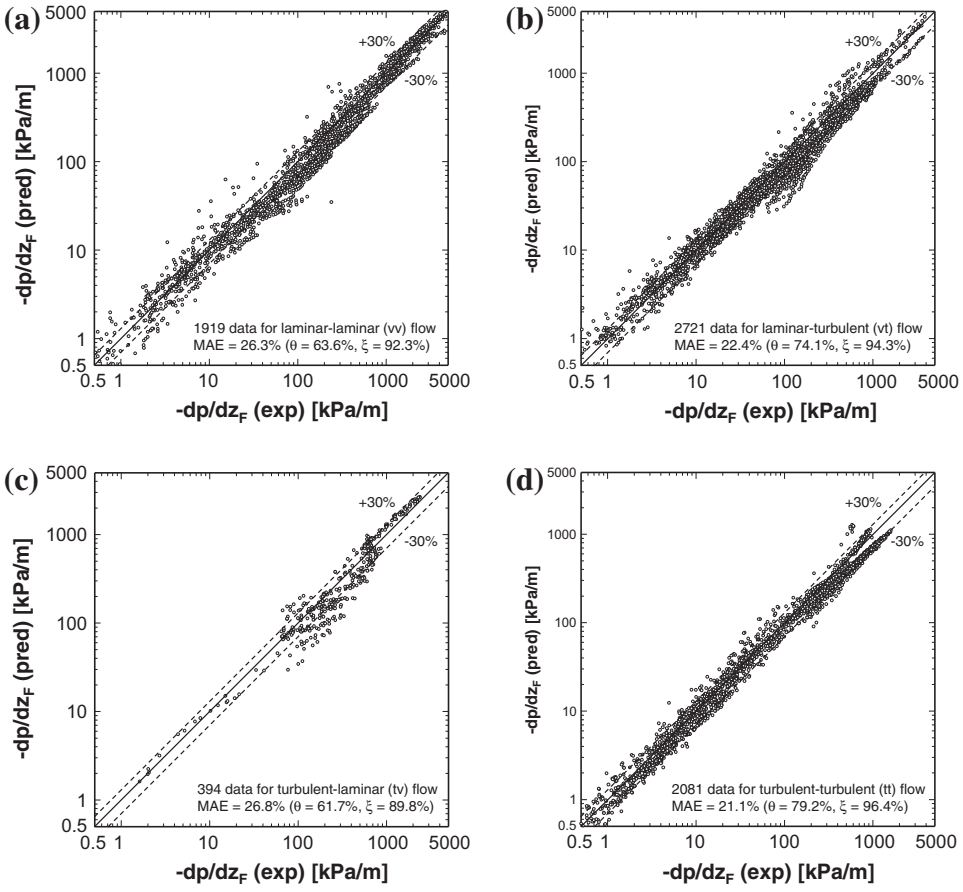

Fig. 7. Comparison of predictions of universal two-phase frictional pressure drop correlation for adiabatic and condensing flows with consolidated 7115 point database for mini/micro-channels with: (a) laminar–laminar (vv) flow, (b) laminar–turbulent (vt) flow, (c) turbulent–laminar (tv) flow, and (d) turbulent–turbulent (tt) flow. (Adapted from [116].)

Table 6
Comparison of individual frictional pressure drop databases with predictions of universal correlation for adiabatic and condensing mini/micro-channel flows and select previous models and correlations [116].

Author(s)	D_h [mm]	Fluid(s)	Test mode	MAE (%)						
				Dukler et al. [91]	Beattie and Whalley [92]	Müller-Steinhagen and Heck [96]	Mishima and Hibiki [99]	Sun and Mishima [106]	Li and Wu [107]	Universal correlation
Hinde et al. [38]	4.57	R134a, R12	Condensation	54.3	47.2	35.4	62.7	38.1	47.2	31.3
Wambsganss et al. [39]	5.44	Air–water	Adiabatic	38.5	39.5	48.5	57.7	46.8	54.1	27.4
Fujita et al. [40]	0.39, 2.14, 3.33	N_2–water, N_2–ethanol	Adiabatic	27.6	52.9	34.5	67.1	37.8	101.8	33.9
Hirofumi and Webb [41]	0.96–2.13	R134a	Adiabatic	23.9	18.1	21.2	55.1	18.5	25.3	25.3
Yang and Webb [42]	2.64	R12, R134a	Adiabatic	45.4	36.7	19.7	50.1	22.7	36.7	14.6
Triplett et al. [43]	1.088, 1.097, 1.447	Air–water	Adiabatic	32.7	24.2	36.6	37.0	28.2	34.0	21.8
Bao et al. [44]	1.95	Air–water	Adiabatic	42.8	21.3	27.1	25.3	29.1	24.2	19.5
Coleman [45]	0.761–4.910	R134a	Adiabatic	36.8	28.4	14.6	41.0	18.0	57.7	15.7
Coleman [45]	0.424–1.524	R134a	Condensation	31.1	21.0	18.8	19.3	16.6	56.0	14.0
Wang et al. [46]	3.0	R410A, R407C, R22	Adiabatic	54.2	47.8	26.2	27.3	38.2	49.8	25.0
Zhang and Webb [47]	2.13, 3.25, 6.20	R134a, R22, R404A	Adiabatic	32.2	23.9	11.7	80.4	13.0	24.5	16.3
Nino et al. [48]	1.02, 1.54	R410A, R134a	Adiabatic	32.4	24.8	21.4	22.6	20.4	63.8	14.8
Nino et al. [48]	1.02, 1.54	Air–water	Adiabatic	21.4	22.5	73.0	44.1	75.2	36.0	22.6
Adams et al. [49]	1.02, 1.54	CO_2, ammonia, R245fa	Adiabatic	24.9	25.6	44.4	46.4	48.1	89.6	29.8
Monroe et al. [50]	1.66	R134a	Adiabatic	48.4	41.1	16.7	23.3	24.6	31.8	24.2
Pehlivan [51]	0.8, 1.0, 3.0	Air–water	Adiabatic	45.5	51.9	52.4	28.8	44.2	32.6	30.9
Jang and Hrnjak [52]	6.10	CO_2	Adiabatic	39.4	31.4	10.6	95.2	20.3	31.4	24.7
Shin [53]	0.493–1.067	R134a	Condensation	44.4	36.5	16.1	24.8	18.6	40.5	23.4
Tu and Hrnjak [54]	0.0695–0.3047	R134a	Adiabatic	23.2	46.7	29.9	21.3	88.7	36.6	18.2
Cavallini et al. [55]	1.4	R410A, R134a, R236ea	Adiabatic	31.8	30.9	33.4	52.2	29.1	27.0	32.9
Chen et al. [56]	3.25	R410A	Adiabatic	35.0	28.5	9.6	76.6	20.7	28.5	21.3
Mitra [57]	6.22	R410A	Condensation	44.0	37.5	26.3	148.2	28.0	37.5	23.0
Andresen [58]	0.76, 1.52, 3.05	R410A	Condensation	26.7	16.8	14.9	103.5	12.4	18.1	11.7
English and Kandlikar [59]	1.018	Air–water	Adiabatic	18.4	11.0	35.6	59.7	31.8	47.7	8.1
Hwang and Kim [60]	0.244, 0.430, 0.792	R134a	Adiabatic	32.1	38.1	51.5	25.0	61.8	56.2	31.4
Yun et al. [61]	1.437	R410A	Adiabatic	43.7	35.5	12.1	18.9	25.7	16.9	11.8
Field and Hrnjak [62]	0.148	R134a, R410A, propane, ammonia	Adiabatic	18.7	26.5	47.5	17.8	76.9	19.0	15.2
Park and Hrnjak [63]	0.89, 3.5, 6.1	CO_2, R410A, R22	Adiabatic	41.2	36.2	25.9	58.2	31.2	42.8	31.0
Revellin and Thome [64]	0.517	R134a, R245fa	Adiabatic	47.1	36.9	27.6	49.8	28.4	21.7	29.1
Yue et al. [65]	0.667	CO_2–water	Adiabatic	54.6	25.7	25.8	33.0	29.1	37.2	25.6
Quan et al. [66]	0.109, 0.142, 0.151	Water	Condensation	27.3	26.1	115.3	16.7	34.9	16.8	20.5
Dutkowski [67]	0.64–2.30	Air–water	Adiabatic	29.5	32.7	32.1	34.1	39.0	35.9	32.1
Marak [68]	1.0	Methane	Condensation	37.7	30.7	17.6	37.8	24.2	31.2	16.2
Park and Hrnjak [69]	0.89	CO_2	Adiabatic	17.0	13.1	29.2	23.1	24.3	104.5	33.7
Huang et al. [70]	1.6, 4.18	R410A	Condensation	48.6	40.5	21.5	56.0	28.0	39.0	18.4
Choi et al. [71]	0.143, 0.322, 0.490	N_2–water	Adiabatic	33.4	40.7	40.6	24.3	41.8	26.5	22.9
Ducoulombier et al. [72]	0.529	CO_2	Adiabatic	37.2	29.2	15.3	25.4	15.3	27.6	14.3
Tibiriçá and Ribatski [73]	2.32	R245fa	Adiabatic	42.8	34.0	14.3	22.8	23.0	36.1	15.7
Total				36.2	33.2	30.1	41.8	33.2	37.7	23.3

Heck overpredicts the data especially for high qualities, while the universal correlation captures the data in both magnitude and trend with better accuracy.

5. Pressure drop in flow boiling

5.1. Consolidation of world databases for flow boiling in mini/micro-channels

A total of 2378 two-phase pressure drop data points for flow boiling in mini/micro-channels were amassed from 16 sources [31,50,73–86]. The database consists of 2033 single-channel data points from 12 sources, and 345 multi-channel data points from 4 sources. Table 7 describes the individual databases comprising the consolidated database. Unlike prior databases, the new consolidated database includes a broad range of reduced pressures, from 0.005 to 0.78.

The 2378 point consolidated database includes 1883 frictional pressure drop data points from 11 sources and 495 total pressure drop data points from 5 sources. As discussed by the authors of the present study [117], the choice of void fraction relation used to determine the accelerational pressure gradient is relatively insignificant compared to the choice of frictional gradient correlation, despite the appreciable axial changes in quality between the channel inlet and outlet. Therefore, for the 495 total pressure drop data points, the frictional pressure drop is isolated by subtracting the accelerational and gravitational gradients calculated using Eqs. (3) and (4), respectively, based on the Zivi void fraction relation, Eq. (5). The remaining 1883 frictional pressure drop data were determined by the original authors by subtracting the accelerational and gravitational pressure drop components from the measured total pressure drop. For example, Huo [77] used the Lockhart and Martinelli [94] void fraction relation,

$$\alpha = \left[1 + 0.28\left(\frac{1-x}{x}\right)^{0.64}\left(\frac{\rho_g}{\rho_f}\right)^{0.36}\left(\frac{\mu_f}{\mu_g}\right)^{0.07}\right]^{-1}, \tag{21}$$

to calculate the accelerational pressure drop, while Maqbool et al. [86] used the Woldesemayat and Ghajar [126] relation

$$\alpha = \frac{J_g}{J_g\left[1+\left(\frac{J_f}{J_g}\right)^{\left(\frac{\rho_g}{\rho_f}\right)^{0.1}}\right] + 2.9\left[\frac{gD_h\sigma(1+\cos\phi)(\rho_f-\rho_g)}{\rho_f^2}\right]^{0.25}(1.22+1.22\sin\phi)^{\frac{p_{atm}}{p}}} \tag{22}$$

and Hu et al. [80], Quibén et al. [81], Ducoulombier [82], Tibiriçá and Ribatski [73], Tibiriçá et al. [83] the Rouhani and Axelsson's [124] relation, Eq. (19). Tran [75], Pettersen [76] and Owhaib et al. [79] used the Zivi [113] relation, Eq. (5). Wu et al. [84] neglected the accelerational pressure drop because of the short length of their test section.

5.2. Assessment of previous frictional pressure gradient correlations against consolidated database for flow boiling in mini/micro-channels

The consolidated database for flow boiling in mini/micro-channels is used to assess the accuracy of previous HEMs and

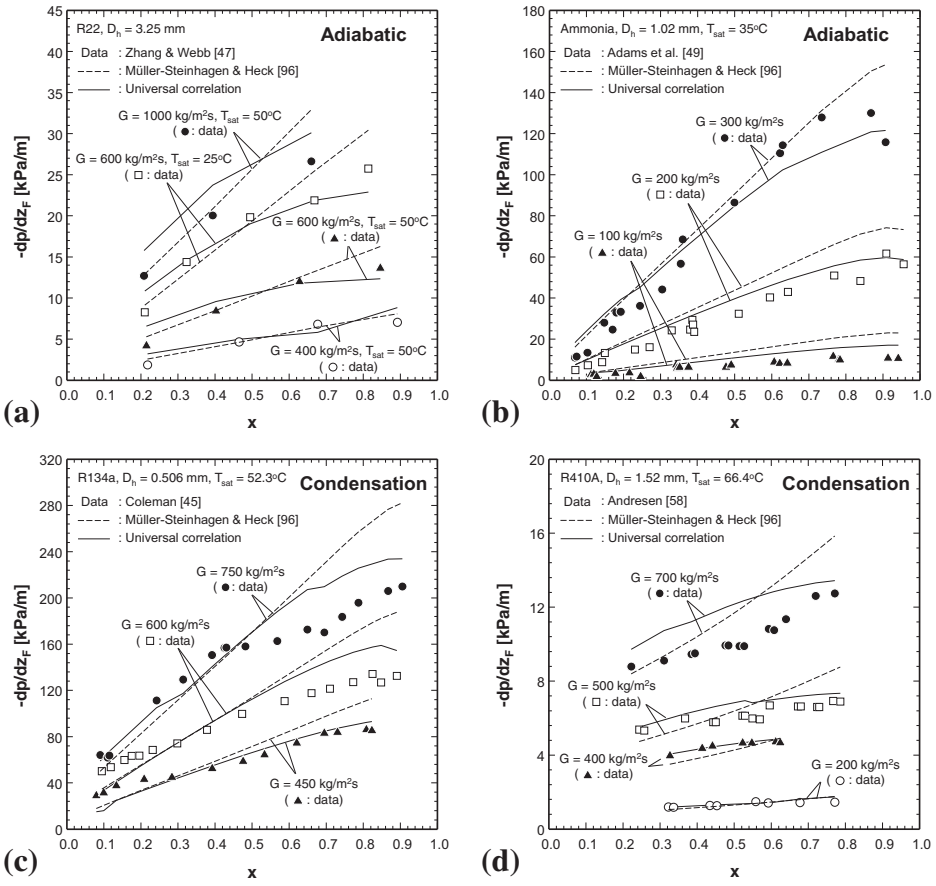

Fig. 8. Comparison of predictions of universal correlation for two-phase frictional pressure drop for adiabatic and condensing mini/micro-channel flows and Müller-Steinhagen and Heck [96] correlation with experimental data for adiabatic mini/micro-channel flow by (a) Zhang and Webb [47] and (b) Adams et al. [49], and condensing mini/micro-channel flow by (c) Coleman [45] and (d) Andresen [58].

Table 7
Two-phase frictional pressure drop data for mini/micro-channel boiling flow included in the consolidated database [117].

Author(s)	Channel geometry[a]	Channel material	D_h [mm]	Fluid(s)	G [kg/m^2 s]	Data type	Data points
Lezzi et al. [74]	C single, H	Stainless steel	1.0	Water	776–2738	Δp_{tp}	86
Tran [75]	C single, H	Brass	2.46	R12, R134a	33–832	$\Delta p_{tp,F}$	439
Pettersen [76]	C multi, H	Aluminum	0.81	CO_2	190–570	$\Delta p_{tp,F}$	57
Monroe et al. [50]	R multi, H	Aluminum	1.66	R134a	99–402	Δp_{tp}	37
Qu and Mudawar [31]	R multi, H	Copper + Lexan cover	0.349	Water	135–402	Δp_{tp}	164
Huo [77]	C single, VU	Stainless steel	2.01, 4.26	R134a	400–500	$\Delta p_{tp,F}$	74
Lee and Mudawar [78]	R multi, H	Copper + Lexan cover	0.349	R134a	128–657	Δp_{tp}	87
Owhaib et al. [79]	C single, VU	Stainless steel	0.826, 1.224, 1.7	R134a	100–400	$\Delta p_{tp,F}$	53
Hu et al. [80]	C single, H	–	2.0, 4.18	R410A	200–620	$\Delta p_{tp,F}$	48
Quibén et al. [81]	R single, H	Copper	3.5, 3.71, 4.88, 5.35	R22, R410A	150–500	$\Delta p_{tp,F}$	264
Ducoulombier [82]	C single, H	Stainless steel	0.529	CO_2	400–1200	$\Delta p_{tp,F}$	268
Tibiriçá and Ribatski [73]	C single, H	Stainless steel	2.32	R245fa	199–701	$\Delta p_{tp,F}$	142
Tibiriçá et al. [83]	C single, H	Stainless steel	2.32	R134a	100–600	$\Delta p_{tp,F}$	49
Wu et al. [84]	C single, H	Stainless steel	1.42	CO_2	300–600	$\Delta p_{tp,F}$	254
Kharangate et al. [85]	R single, H/VU	Copper bottom + Lexan	3.33	FC72	177–1652	Δp_{tp}	121
Maqbool et al. [86]	C single, VU	Stainless steel	1.224, 1.70	Ammonia	100–500	$\Delta p_{tp,F}$	235
Total							2378

[a] C: circular, R: rectangular, H: horizontal, VU: vertical upflow.

semi-empirical correlations in predicting the two-phase frictional pressure gradient using Eqs. (10) and (12), respectively. Table 4 compares the 2378 frictional pressure gradient data points for mini/micro-channel flow boiling with predictions of previous HEMs [87–93], semi-empirical correlations for macro-channels [94–98], and semi-empirical correlations for mini/micro-channels [42,60,99–109]. The viscosity models generally underpredict the mini/micro-channel boiling data, especially those of McAdams et al. [87], Dukler et al. [91], Beattie and Whalley [92] and Lin et al. [93]. Among the semi-empirical correlations, relatively good predictions are achieved using the Müller-Steinhagen and Heck [96] and Mishima and Hibiki [99] correlations, evidenced by MAEs of 31.2% and 27.6%, respectively.

Fig. 9 compares the 2378 mini/micro-channel flow boiling data points with predictions of select HEMs, as well as semi-empirical correlations that have shown relatively superior predictive capability. The viscosity models by Dukler et al. [91], and Beattie and Whalley [92] highly underpredict most of the flow boiling mini/

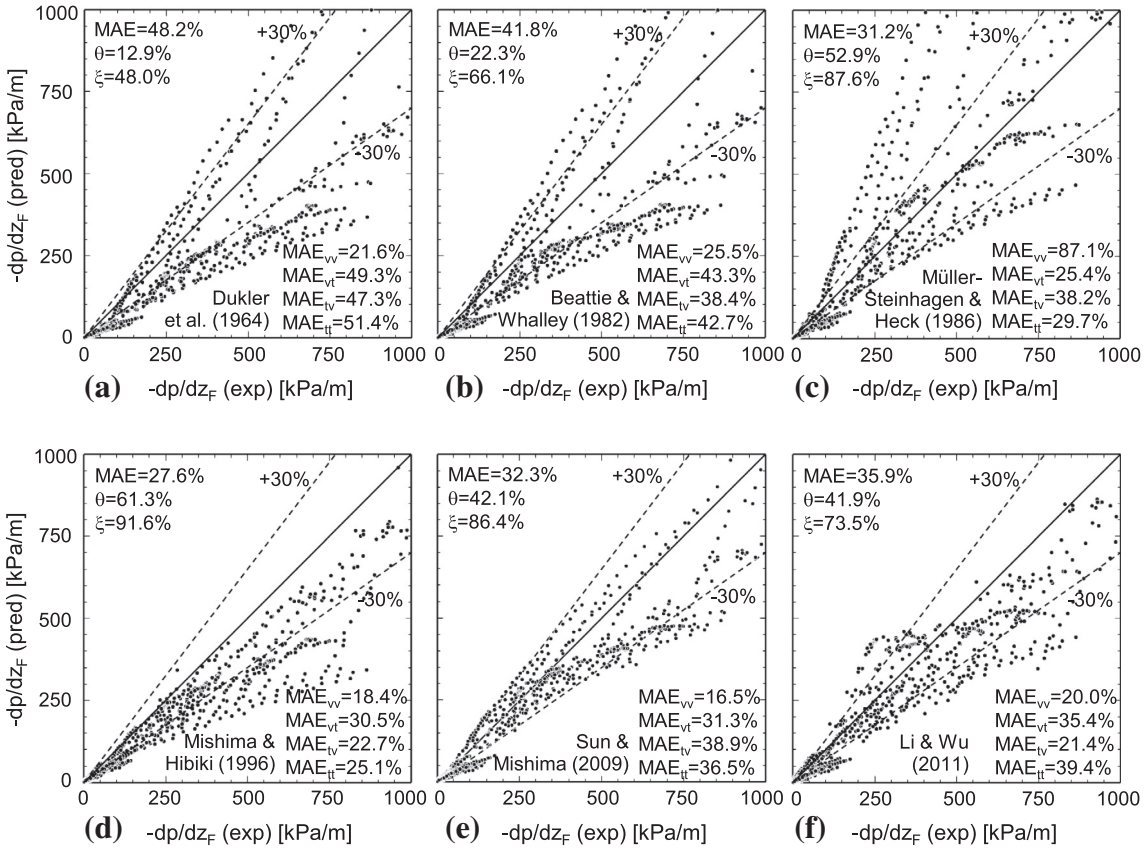

Fig. 9. Comparison of 2378 point consolidated database for frictional pressure gradient in boiling mini/micro-channel flow with predictions of HEM using mixture viscosity models of (a) Dukler et al. [91] and (b) Beattie and Whalley [92], and semi-empirical correlations of (c) MÜller-Steinhagen and Heck [96], (d) Mishima and Hibiki [99], (e) Sun and Mishima [106], and (f) Li and Wu [107]. (Adapted from [117].)

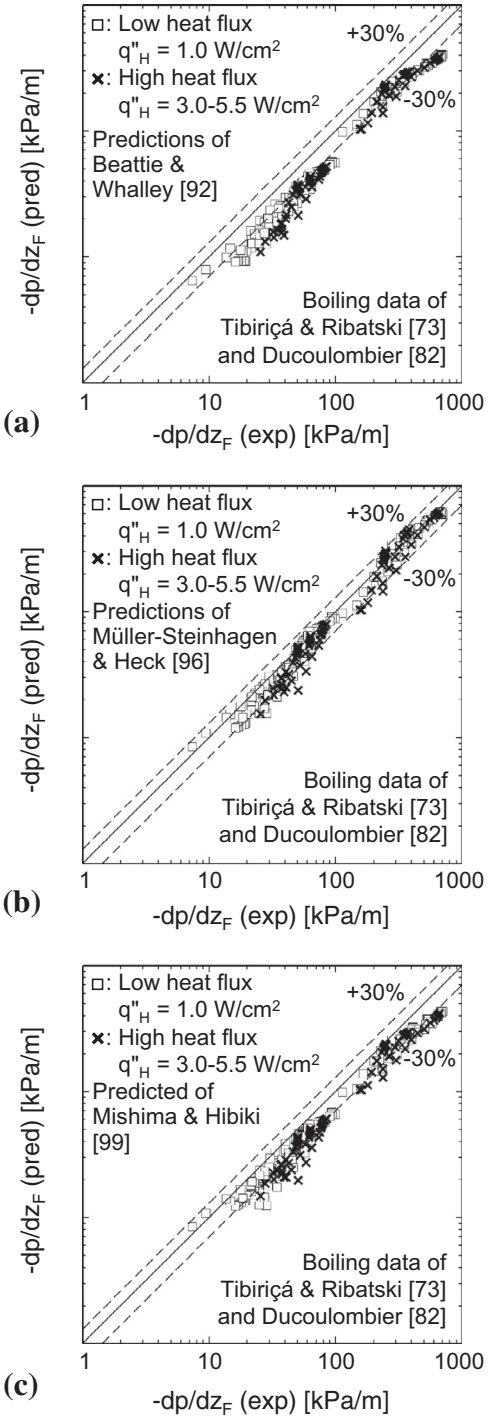

Fig. 10. Comparison of boiling data of Tibiriçá & Ribatski [73] and Ducoulombier [82] corresponding to different heat fluxes with predictions of (a) HEM with viscosity model of Beattie and Whalley [92], and semi-empirical correlations of (b) Müller-Steinhagen and Heck [96] and (c) Mishima and Hibiki [99].

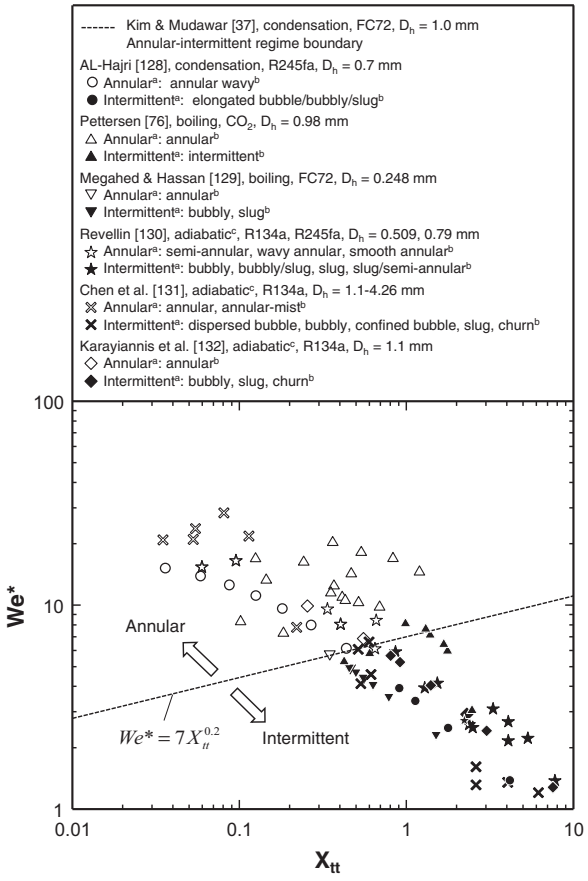

Fig. 11. Flow regime transition between annular and intermittent flows in two-phase condensing, adiabatic, and boiling mini/micro-channel flows. *a*: flow regime terminologies in present study, *b*: flow regime terminologies by original author (s), and *c*: flow regime identification using adiabatic glass observation tube downstream of boiling section. (See above-mentioned references for further information.)

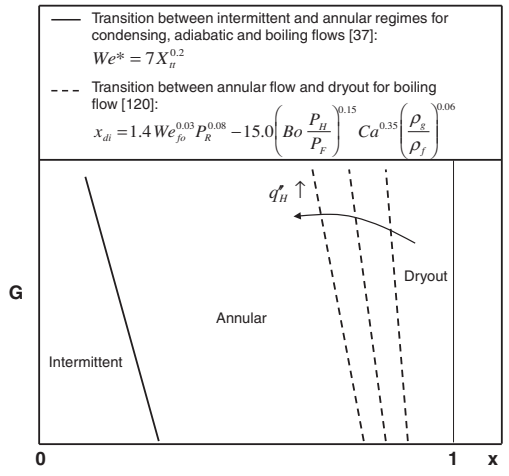

Fig. 12. Qualitative representation of flow regime transitions in two-phase condensing, adiabatic and boiling mini/micro-channel flows.

micro-channel data. The correlation of Müller-Steinhagen and Heck [96] highly overpredicts the data in the laminar-laminar (*vv*) regime, and underpredicts the data in the other flow regimes (*vt*, *tv*, *tt*). Most of the consolidated database is also underpredicted by the mini/micro-channel correlations of Mishima and Hibiki [99], Sun and Mishima [106] and Li and Wu [107].

5.3. Universal predictive method based on consolidated database for flow boiling in mini/micro-channels

As discussed by the present authors [117], the previous models and semi-empirical correlations show different trends when

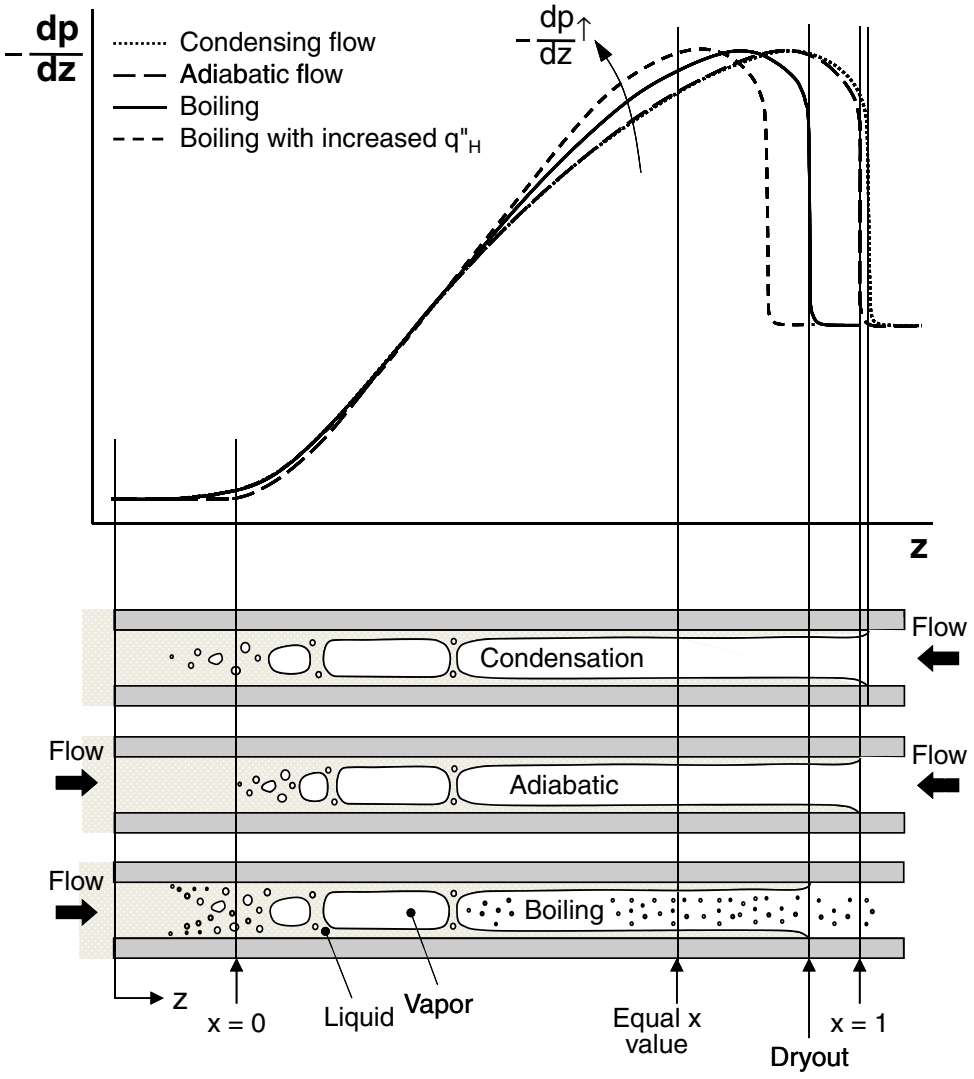

Fig. 13. Schematic representation of pressure gradient variations in two-phase condensing, adiabatic, and boiling flows.

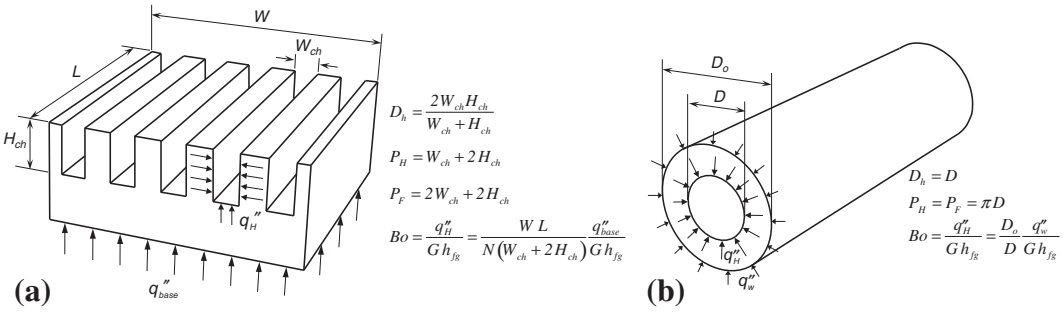

Fig. 14. (a) Rectangular multi-channel heat sink with three-sided wall heating, and (b) circular single channel with uniform circumferential wall heating.

predicting non-boiling versus boiling mini/micro-channel data; moderate or sometimes significant underprediction of the boiling data is observed compared to the non-boiling data. And, for flow boiling, increasing the heat flux intensifies the deviation between data and predictions of a given model or correlation. The heat flux influence is depicted in Fig. 10, which compares the boiling data of Ducoulombier [82] and Tibiriçá and Ribatski [73] with predictions of the HEM using the viscosity relation of Beattie and Whalley [92], Fig. 10(a), and the semi-empirical correlations of Müller-Steinha-

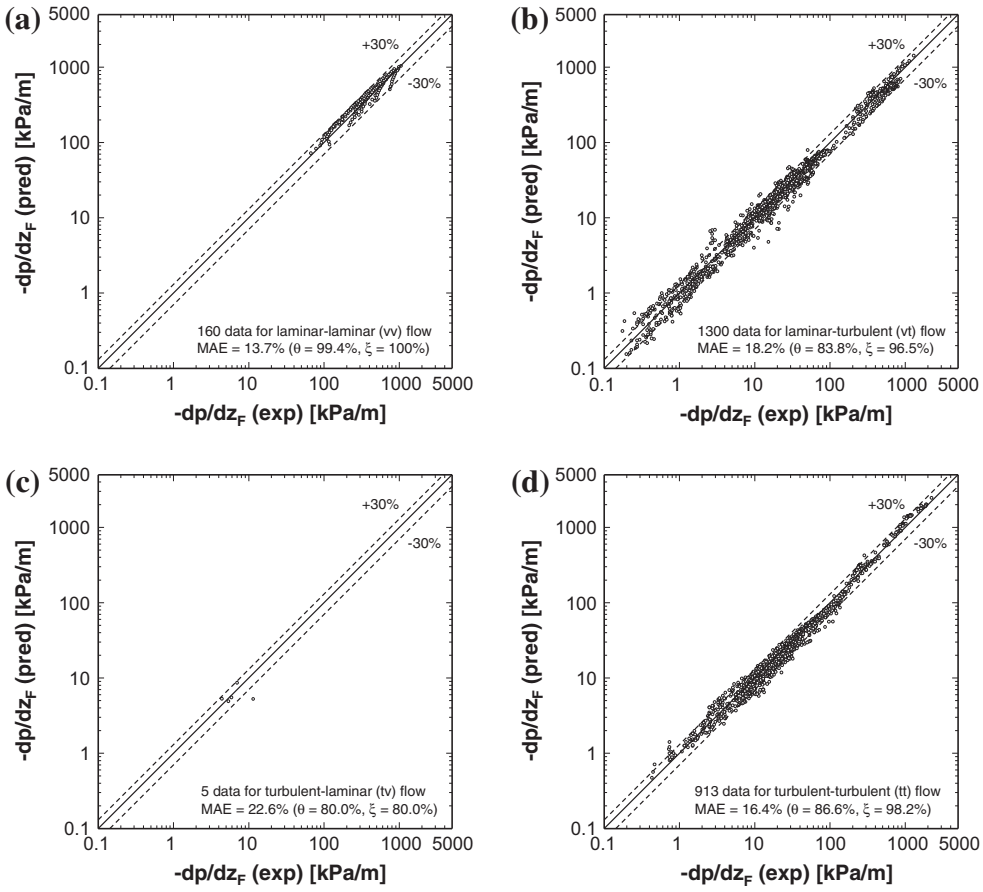

Fig. 15. Comparison of predictions of universal two-phase frictional pressure drop correlation for flow boiling with consolidated 2378 point mini/micro-channel flow boiling database for: (a) laminar-laminar (*vv*) flow, (b) laminar-turbulent (*vt*) flow, (c) turbulent-laminar (*tv*) flow, and (d) turbulent-turbulent (*tt*) flow. (Adapted from [117].)

gen and Heck [96], Fig. 10(b) and Mishima and Hibiki [99], Fig. 10(c).

One method to investigating the differences in predictive accuracy between boiling and non-boiling mini/micro-channel flows by the same model or correlation is to explore the differences in flow regime. In a previous study by the present authors involving condensation of FC-72 along square micro-channels [36], five distinct flow regimes were identified: smooth-annular, wavy-annular, transition, slug, and bubbly. Using a modified Weber number recommended by Soliman [127], flow regime data were segregated into annular (smooth-annular, wavy-annular, and transition) for $We^* > 7X_{tt}^{0.2}$ and intermittent (slug, and bubbly) for $We^* < 7X_{tt}^{0.2}$ [37], where

$$We^* = 2.45\frac{Re_g^{0.64}}{Su_{go}^{0.3}\left(1+1.09X_{tt}^{0.039}\right)^{0.4}} \quad \text{for } Re_f \leqslant 1250 \tag{23a}$$

and

$$We^* = 0.85\frac{Re_g^{0.79}X_{tt}^{0.157}}{Su_{go}^{0.3}\left(1+1.09X_{tt}^{0.039}\right)^{0.4}}\left[\left(\frac{\mu_g}{\mu_f}\right)^2\left(\frac{\upsilon_g}{\upsilon_f}\right)\right]^{0.084} \quad \text{for } Re_f > 1250. \tag{23b}$$

To further examine flow regime transitions, mini/micro-channel data for condensing, boiling and adiabatic flows are plotted in Fig. 11 in terms of the modified Weber number, We^*, and Lockhart–Martinelli parameter, X_{tt}, with clear segregation between the annular data (open symbols) and intermittent data (solid symbols). The boundary of $We^* = 7X_{tt}^{0.2}$ between the annular and intermittent flow regimes from [37] predicts well the mini/micro-channel data for condensing, boiling and adiabatic flows. This implies that there are no differences in annular-intermittent regime boundary among condensing, boiling and adiabatic flows.

Fig. 12 qualitatively summarizes important flow regime boundaries plotted in terms of mass velocity, G, and thermodynamic equilibrium quality, x, encountered in two-phase condensing, adiabatic and boiling mini/micro-channel flows. Unlike condensing and adiabatic flows, partial annular liquid film dryout is expected in flow boiling, where the heat transfer coefficient begins to decrease sharply. The dryout incipience quality decreases with increasing wall heat flux. The correlation for dryout heat flux was developed by the present authors [120] based on a consolidated world database consisting of 997 data points from 26 sources.

Based on the finding from the flow regime transitions, pressure gradient variations for condensing, adiabatic, and boiling flows, and corresponding flow regimes are illustrated schematically in Fig. 13. The highest pressure gradient is expected at a location within the annular flow regime. With the assumption that the same flow regimes are encountered at the same local liquid and vapor (or gas) flow rates, a given x value that yields annular flow for adiabatic and condensing flows should also yield annular flow for boiling flow. However, there are fundamental differences in annular flow structure stemming from liquid droplet entrainment. For boiling flow, droplets are formed upstream by shattering of the liquid ridges between slug flow bubbles. These droplets persist in the vapor core even downstream of the wall dryout location. On the other hand, pure vapor (or gas) flow at the inlet in condensing and adiabatic flows renders such liquid droplet entrainment effects far less likely. As illustrated in Fig. 13, there is a shift in the location

Table 8
Universal two-phase frictional pressure gradient correlation for flow boiling in mini/micro-channels in both single- and multi-channel configurations [117]. The non-boiling pressure gradient correlations for adiabatic and condensing flows are included in Table 5.

$\left(\frac{dp}{dz}\right)_F = \left(\frac{dp}{dz}\right)_f \phi_f^2$

where $\phi_f^2 = 1 + \frac{C}{X} + \frac{1}{X^2}, X^2 = \frac{(dp/dz)_f}{(dp/dz)_g}$

$-\left(\frac{dp}{dz}\right)_f = \frac{2f_f v_f G^2 (1-x)^2}{D_h}, \quad -\left(\frac{dp}{dz}\right)_g = \frac{2f_g v_g G^2 x^2}{D_h}$

$f_k = 16Re_k^{-1}$ for $Re_k < 2000$

$f_k = 0.079Re_k^{-0.25}$ for $2000 \leqslant Re_k < 20{,}000$

$f_k = 0.046Re_k^{-0.2}$ for $Re_k \geqslant 20{,}000$

for laminar flow in rectangular channels:

$f_k Re_k = 24\left(1 - 1.3553\beta + 1.9467\beta^2 - 1.7012\beta^3 + 0.9564\beta^4 - 0.2537\beta^5\right)$

where subscript k denotes f or g for liquid and vapor phases, respectively,

$Re_f = \frac{G(1-x)D_h}{\mu_f}, \quad Re_g = \frac{GxD_h}{\mu_g}, \quad Re_{fo} = \frac{GD_h}{\mu_f}, \quad Su_{go} = \frac{\rho_g \sigma D_h}{\mu_g^2}, \quad We_{fo} = \frac{G^2 D_h}{\rho_f \sigma}, \quad Bo = \frac{q''_H}{Gh_{fg}}$

q''_H: effective heat flux averaged over heated perimeter of channel, P_H: heated perimeter of channel, P_F: wetted perimeter of channel

	$C_{non\text{-}boiling}$
$Re_f \geqslant 2000$, $Re_g \geqslant 2000$ (tt)	$0.39Re_{fo}^{0.03} Su_{go}^{0.10} \left(\frac{\rho_f}{\rho_g}\right)^{0.35}$
$Re_f \geqslant 2000$, $Re_g < 2000$ (tv)	$8.7 \times 10^{-4} Re_{fo}^{0.17} Su_{go}^{0.50} \left(\frac{\rho_f}{\rho_g}\right)^{0.14}$
$Re_f < 2000$, $Re_g \geqslant 2000$ (vt)	$0.0015Re_{fo}^{0.59} Su_{go}^{0.19} \left(\frac{\rho_f}{\rho_g}\right)^{0.36}$
$Re_f < 2000$, $Re_g < 2000$ (vv)	$3.5 \times 10^{-5} Re_{fo}^{0.44} Su_{go}^{0.50} \left(\frac{\rho_f}{\rho_g}\right)^{0.48}$
	C
$Re_f \geqslant 2000$	$C_{non-boiling}\left[1 + 60We_{fo}^{0.32}\left(Bo\frac{P_H}{P_F}\right)^{0.78}\right]$
$Re_f < 2000$	$C_{non-boiling}\left[1 + 530We_{fo}^{0.52}\left(Bo\frac{P_H}{P_F}\right)^{1.09}\right]$

Correlation based on consolidated database of 2378 boiling pressure drop data points from 16 sources with the following application range:
- Working fluid: R12, R134a, R22, R245fa, R410A, FC-72, ammonia, CO_2, and water
- Hydraulic diameter: $0.349 < D_h < 5.35$ mm
- Mass velocity: $33 < G < 2738$ kg/m^2 s
- Liquid-only Reynolds number: $156 < Re_{fo} = GD_h/\mu_f < 28{,}010$
- Superficial liquid Reynolds number: $0 < Re_f = G(1-x)D_h/\mu_f < 16{,}020$
- Superficial vapor Reynolds number: $0 < Re_g = GxD_h/\mu_g < 199{,}500$
- Flow quality: $0 < x < 1$
- Reduced pressure: $0.005 < P_R < 0.78$

where $x = 0$ for boiling flow because of non-equilibrium effects downstream of the dryout location. A corresponding shift in the span of the annular film in the same region causes a shift in the location of maximum pressure gradient for boiling flow compared to condensing and adiabatic flows. Moreover, both locations of wall dryout and maximum pressure gradient for boiling flow move upstream with increasing heat flux. These trends clearly point to the need to utilize different predictive tools for pressure gradient in boiling flow compared to condensing and adiabatic flows.

To account for differences in local frictional pressure gradient between boiling and non-boiling mini/micro-channel flows, the C function in the Lockhart–Martinelli parameter for non-boiling mini/micro-channel flows was modified by the Weber and Boiling numbers. In the modified function, the ratio of the flow channel's heated to wetted perimeters, P_H/P_F, is also considered to cope with non-uniform circumferential heat flux. The definitions of P_H, P_F and Boiling number for three-sided wall heating for a multi-channel heat sink with rectangular channels that are fitted atop with an insulating cover plate, and for a single circular channel with uniform circumferential wall heating are illustrated in Fig. Fig. 14(a) and (b), respectively. Fig. 15 shows the universal two-phase frictional pressure gradient correlation for flow boiling, which is summarized in Table 8, predicts the entire 2378 point consolidated mini/micro-channel database quite accurately, evidenced by MAEs of 13.7%, 18.1%, 22.6%, and 16.4% for *vv, vt, tv, tt* flow regimes, respectively [117].

The predictive accuracy of the universal correlation is also examined in Table 9 by comparing individual mini/micro-channel databases from 16 sources with predictions of the universal correlation as well as select previous models and correlations. Among the previous predictive tools, only the correlation of Mishima and Hibiki [99] provides fair predictions, but with most of the boiling data underpredicted. The universal correlation provides excellent predictions against all individual databases, with 12 databases predicted more accurately than any of the select previous models or correlations, and the best overall MAE of 17.2%, with 85.9% and 97.4% of the data falling within ±30% and ±50% error bands, respectively.

Predictions of the universal correlation and Müller-Steinhagen and Heck's [96] correlation are compared in Fig. 16 with representative boiling data [73,85]. While the Müller-Steinhagen and Heck underpredicts most of the boiling data, the universal correlation accurately predicts the pressure gradient data in both magnitude and trend.

5.4. Recommendations for future work

The success of the two universal correlations in predicting the frictional pressure gradient for adiabatic, condensing and boiling micro-channel flows points to the need to begin shifting research focus to both theoretical and computational models. This shift has been very successful for single-phase mini/micro-channel flows [133], but is highly complicated for two-phase flows because of poor understanding of interfacial behavior. For example, accurate modeling of the annular flow regime, which is responsible for both the highest pressure gradient and highest heat transfer coefficient, is highly dependant on accurate temporal and spatial measurements of both liquid film thickness and liquid velocity profile. While such measurements have been successfully accomplished in macro systems [134,135], small channel size in mini/

Table 9
Comparison of individual databases with predictions of universal correlation for frictional pressure drop in mini/micro-channel boiling flow and select previous correlations [117].

Author(s)	D_h [mm]	Fluid(s)	Mean absolute error (%)						
			Dukler et al. [91]	Beattie and Whalley [92]	Müller-Steinhagen and Heck [96]	Mishima and Hibiki [99]	Sun and Mishima [106]	Li and Wu [107]	Universal correlation
Lezzi et al. [74]	1.00	Water	33.5	29.7	13.3	18.8	26.5	13.0	15.6
Tran [75]	2.46	R12, R134a	53.9	45.5	32.6	32.0	35.0	46.4	20.0
Pettersen [76]	0.81	CO_2	55.4	47.6	37.7	29.4	38.1	24.1	29.7
Monroe et al. [50]	1.66	R134a	48.7	42.4	19.4	24.3	26.7	23.6	24.2
Qu and Mudawar [31]	0.349	Water	22.1	26.0	88.1	18.4	16.3	20.0	13.6
Huo [77]	2.01, 4.26	R134a	73.4	67.9	61.0	31.0	61.9	70.4	20.2
Lee and Mudawar [78]	0.349	R134a	43.7	39.8	26.8	42.9	21.2	28.4	16.2
Owhaib et al. [79]	0.826, 1.224, 1.70	R134a	40.6	29.8	26.6	19.0	26.6	53.9	18.1
Hu et al. [80]	2.00, 4.18	R410A	45.0	38.7	18.8	16.5	27.6	38.2	15.2
Quibén et al. [81]	3.5, 3.71, 4.88, 5.35	R22, R410A	49.9	43.4	21.8	25.8	34.2	43.4	20.2
Ducoulombier [82]	0.529	CO_2	39.7	32.0	13.3	27.7	16.3	25.5	13.4
Tibiriçá and Ribatski [73]	2.32	R245fa	48.1	40.7	13.6	20.3	26.0	46.1	7.9
Tibiriçá et al. [83]	2.32	R134a	59.9	53.7	34.9	19.8	41.8	56.1	12.3
Wu et al. [84]	1.42	CO_2	54.6	48.1	30.6	29.5	38.6	24.2	19.0
Kharangate et al. [85]	3.33	FC72	52.6	47.2	42.5	30.5	43.9	47.2	15.5
Maqbool et al. [86]	1.224, 1.700	Ammonia	51.6	42.6	27.3	30.9	42.4	27.4	17.1
Total			48.2	41.8	31.2	27.6	32.3	35.9	17.2

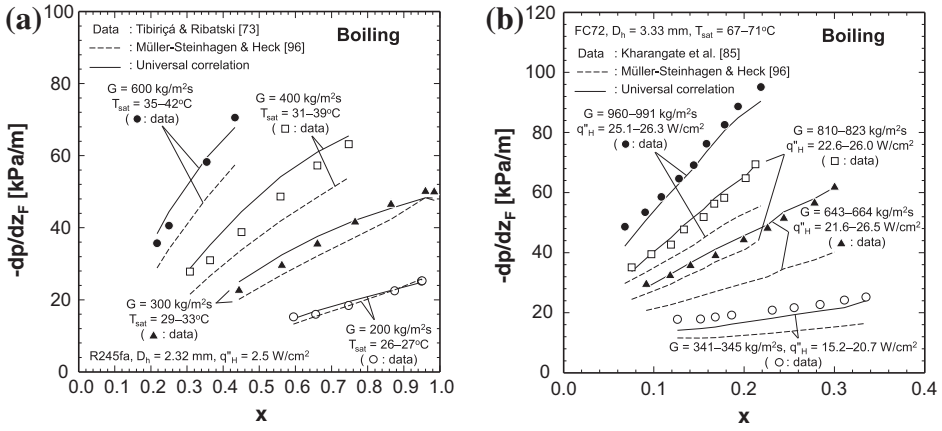

Fig. 16. Comparison of predictions of universal correlation for frictional pressure gradient in mini/micro-channel flow boiling and Müller-Steinhagen and Heck [96] correlation with experimental data by (a) Tibiriçá and Ribatski [73] and (b) Kharangate et al. [85].

micro-channels poses major challenges that will require new sophisticated methods that are specifically tailored to small channels.

6. Conclusions

This study reviewed methods for determining the frictional pressure gradient in adiabatic, condensing and boiling mini/micro-channel flows. It was shown that two key difficulties in selecting a suitable model or correlation are limited validity to a few working fluids and narrow ranges of operating conditions. This limitation was addressed with the development of two consolidated mini/micro-channel databases, one for adiabatic and condensing flows, and the other for boiling flow. Key findings from the study are as follows:

1. There are fundamental differences in flow structure between adiabatic and condensing mini/micro-channels flows on one hand and boiling flow on the other. These differences, which stem from liquid droplet entrainment effects, require the use of different predictive methods for adiabatic and condensing flows versus boiling flow.
2. Two separate consolidated mini/micro-channel databases are discussed. The first is for adiabatic and condensing flows, and consists of 7115 frictional pressure gradient data points from 36 sources, and the second for boiling flow, and consists of 2378 data points from 16 sources. These databases encompass a large number of fluids and very broad ranges of operating conditions.
3. The consolidated databases are shown to be effective tools for assessing the accuracy of previous models and correlations as well as for development of 'universal' correlations that are applicable to a large number of fluids and very broad ranges of operating conditions.

Conflict of interest

None declared.

Acknowledgment

The authors are grateful for the support for this project from the National Aeronautics and Space Administration (NASA) under Grant No. NNX13AC83G.

References

[1] I. Mudawar, Assessment of high-heat-flux thermal management schemes, IEEE Trans-CPMT: Compon. Packag. Technol. 24 (2001) 122–141.
[2] I. Mudawar, Two-phase micro-channel heat sinks: theory, applications and limitations, J. Electron. Packag.-Trans. ASME 133 (2011) 041002-2.
[3] T.M. Anderson, I. Mudawar, Microelectronic cooling by enhanced pool boiling of a dielectric fluorocarbon liquid, J. Heat Transfer – Trans. ASME 111 (1989) 752–759.
[4] I. Mudawar, A.H. Howard, C.O. Gersey, An analytical model for near-saturated pool boiling CHF on vertical surfaces, Int. J. Heat Mass Transfer 40 (1997) 2327–2339.
[5] I. Mudawar, D.E. Maddox, Critical heat flux in subcooled flow boiling of fluorocarbon liquid on a simulated chip in a rectangular channel, Int. J. Heat Mass Transfer 32 (1989) 379–394.
[6] T.C. Willingham, I. Mudawar, Forced-convection boiling and critical heat flux from a linear array of discrete heat sources, Int. J. Heat Mass Transfer 35 (1992) 2879–2890.
[7] T.N. Tran, M.W. Wambsganss, D.M. France, Small circular- and rectangular-channel boiling with two refrigerants, Int. J. Multiphase Flow 22 (1996) 485–498.
[8] H.J. Lee, S.Y. Lee, Heat transfer correlation for boiling flows in small rectangular horizontal channels with low aspect ratios, Int. J. Multiphase Flow 27 (2001) 2043–2062.
[9] Y. Katto, M. Kunihiro, Study of the mechanism of burn-out in boiling system of high burn-out heat flux, Bull. JSME 16 (1973) 1357–1366.
[10] M. Monde, T. Inoue, Critical heat flux in saturated forced convective boiling on a heated disk with multiple impinging jets, J. Heat Transfer – Trans. ASME 113 (1991) 722–727.
[11] D.C. Wadsworth, I. Mudawar, Enhancement of single-phase heat transfer and critical heat flux from an ultra-high-flux-source to a rectangular impinging jet of dielectric liquid, J. Heat Transfer – Trans. ASME 114 (1992) 764–768.
[12] M.E. Johns, I. Mudawar, An ultra-high power two-phase jet-impingement avionic clamshell module, J. Electron. Packag.-Trans. ASME 118 (1996) 264–270.
[13] S. Toda, A study in mist cooling (1st report: investigation of mist cooling), Trans. JSME 38 (1972) 581–588.
[14] L. Lin, R. Ponnappan, Heat transfer characteristics of spray cooling in a closed loop, Int. J. Heat Mass Transfer 46 (2003) 3737–3746.
[15] M. Visaria, I. Mudawar, Theoretical and experimental study of the effects of spray orientation on two-phase spray cooling and critical heat flux, Int. J. Heat Mass Transfer 51 (2008) 2398–2410.
[16] P.J. Marto, V.J. Lepere, Pool boiling heat transfer from enhanced surfaces to dielectric fluids, J. Heat Transfer – Trans. ASME 104 (1982) 292–299.
[17] W. Nakayama, T. Nakajima, S. Hirasawa, Heat sink studs having enhanced boiling surfaces for cooling of microelectronic components, ASME Paper 84-WA/HT-89, 1984.
[18] R.L. Webb, The evolution of enhanced surface geometries for nucleate boiling, Heat Transfer Eng. 2 (1981) 46–69.
[19] V. Khanikar, I. Mudawar, T. Fisher, Effects of carbon nanotube coating on flow boiling in a micro-channel, Int. J. Heat Mass Transfer 52 (2009) 3805–3817.
[20] M.K. Sung, I. Mudawar, Experimental and numerical investigation of single-phase heat transfer using a hybrid jet-impingement/micro-channel cooling scheme, Int. J. Heat Mass Transfer 49 (2006) 682–694.
[21] M.K. Sung, I. Mudawar, Correlation of critical heat flux in hybrid jet impingement/micro-channel cooling scheme, Int. J. Heat Mass Transfer 49 (2006) 2663–2672.
[22] I. Mudawar, M.A. El-Masri, C.S. Wu, J.R. Ausman-Mudawar, Boiling heat transfer and critical heat flux in high-speed rotating liquid films, Int. J. Heat Mass Transfer 28 (1985) 795–806.
[23] J.C. Sturgis, I. Mudawar, Assessment of CHF enhancement mechanisms in a curved, rectangular channel subjected to concave heating, J. Heat Transfer – Trans. ASME 121 (1999) 394–404.
[24] A.P. Ornatskii, L.S. Vinyarskii, Heat transfer crisis in a forced flow of underheated water in small-bore tubes, Teplofizika Vysokikh Temperatur 3 (1965) 444–451.
[25] D.D. Hall, I. Mudawar, Ultra-high critical heat flux (CHF) for subcooled water flow boiling – II: High-CHF database and design parameters, Int. J. Heat Mass Transfer 42 (1999) 1429–1456.
[26] P.E. Jimenez, I. Mudawar, A multi-kilowatt immersion-cooled standard electronic clamshell module for future aircraft avionics, J. Electron. Packag. – Trans. ASME 116 (1994) 220–229.
[27] T.J. LaClair, I. Mudawar, Thermal transients in a capillary evaporator prior to the initiation of boiling, Int. J. Heat Mass Transfer 43 (2000) 3937–3952.
[28] I. Mudawar, D. Bharathan, K. Kelly, S. Narumanchi, Two-phase spray cooling of hybrid vehicle electronics, IEEE Trans. – Compon. Packag. Manuf. Technol. 32 (2009) 501–512.
[29] I. Mudawar, Micro-channel heat exchangers for metal hydride hydrogen storage systems, US Provisional Patent Application No. 61/184,595, 2009.
[30] M.B. Bowers, I. Mudawar, High flux boiling in low flow rate, low pressure drop mini-channel and micro-channel heat sinks, Int. J. Heat Mass Transfer 37 (1994) 321–332.
[31] W. Qu, I. Mudawar, Measurement and prediction of pressure drop in two-phase micro-channel heat sinks, Int. J. Heat Mass Transfer 46 (2003) 2737–2753.
[32] Y. Gan, J. Xu, S. Wang, Are the available boiling heat transfer coefficients suitable for silicon microchannel heat sinks?, Microfluids Nanofluids 4 (2008) 575–587
[33] H.Y. Wu, P. Cheng, Boiling instability in parallel silicon microchannels at different heat flux, Int. J. Heat Mass Transfer 47 (2004) 3631–3641.
[34] G. Wang, P. Cheng, A.E. Bergles, Effects of inlet/outlet configurations on flow boiling instability in parallel microchannels, Int. J. Heat Mass Transfer 51 (2008) 2267–2281.
[35] L. Jiang, M. Wong, Y. Zohar, Phase change in microchannel heat sinks with integrated temperature sensors, J. Microelectromech. Syst. 8 (1999) 358–365.
[36] S.M. Kim, J. Kim, I. Mudawar, Flow condensation in parallel micro-channels – Part 1: Experimental results and assessment of pressure drop correlations, Int. J. Heat Mass Transfer 55 (2012) 971–983.
[37] S.M. Kim, I. Mudawar, Flow condensation in parallel micro-channels – Part 2: Heat transfer results and correlation technique, Int. J. Heat Mass Transfer 55 (2012) 984–994.
[38] D.K. Hinde, M.K. Dobson, J.C. Chato, M.E. Mainland, N. Rhines, Condensation of refrigerants 12 and 134a in horizontal tubes with and without oil, Report No. ACRC TR-26, Air Conditioning and Refrigeration Center, University of Illinois at Urbana-Champaign, 1992.
[39] M.W. Wambsganss, J.A. Jendzejczky, D.M. France, N.T. Obot, Frictional pressure gradients in two-phase flow in a small horizontal rectangular channel, Exp. Therm. Fluid Sci. 5 (1992) 40–56.
[40] H. Fujita, T. Ohara, M. Hirota, H. Furuta, Gas-liquid flows in flat channels with small channel clearance, Adv. Multiphase Flow (1995) 441–451.
[41] H. Hirofumi, R.L. Webb, Condensation in extruded aluminum tubes, Penn State Research Report, Showa Aluminum Corporation, 1995.
[42] C.Y. Yang, R.L. Webb, Friction pressure drop of R-12 in small hydraulic diameter extruded aluminum tubes with and without micro-fins, Int. J. Heat Mass Transfer 39 (1996) 801–809.
[43] K.A. Triplett, S.M. Ghiaasiaan, S.I. Abdel-Khalik, A. LeMouel, B.N. McCord, Gas–liquid two-phase flow in microchannels – Part II: void fraction and pressure drop, Int. J. Multiphase Flow 25 (1999) 395–410.
[44] Z.Y. Bao, D.F. Fletcher, B.S. Haynes, An experimental study of gas–liquid flow in a narrow conduit, Int. J. Heat Mass Transfer 43 (2000) 2313–2324.
[45] J.W. Coleman, Flow visualization and pressure drop for refrigerant phase change and air-water flow in small hydraulic diameter geometries (Ph.D. thesis), Iowa State University, IA, 2000.
[46] C.C. Wang, S.K. Chiang, Y.J. Chang, T.W. Chung, Two-phase flow resistance of refrigerants R-22, R-410A and R-407C in small diameter tubes, Trans. IChemE 79 (2001) 553–560.
[47] M. Zhang, R.L. Webb, Correlation of two-phase friction for refrigerants in small-diameter tubes, Exp. Therm. Fluid Sci. 25 (2001) 131–139.
[48] V.G. Nino, P.S. Hrnjak, T.A. Newell, Characterization of two-phase flow in microchannels, Report No. ACRC TR-202, Air Conditioning and Refrigeration Center, University of Illinois at Urbana-Champaign, 2002.
[49] D.C. Adams, P.S. Hrnjak, T.A. Newell, Pressure drop and void fraction in microchannels using carbon dioxide, ammonia, and R245fa as refrigerants, Report No. ACRC TR-221, Air Conditioning and Refrigeration Center, University of Illinois at Urbana-Champaign, 2003.
[50] C.A. Monroe, T.A. Newell, J.C. Chato, An experimental investigation of pressure drop and heat transfer in internally enhanced aluminum microchannels, Report No. ACRC TR-213, Air Conditioning and Refrigeration Center, University of Illinois at Urbana-Champaign, 2003.
[51] K.K. Pehlivan, Experimental study on two-phase flow regimes and frictional pressure drop in mini- and micro-channels (MS thesis), Concordia University, Canada, 2003.
[52] J. Jang, P.S. Hrnjak, Condensation of CO_2 at low temperature, Report No. ACRC CR-56, Air Conditioning and Refrigeration Center, University of Illinois at Urbana-Champaign, 2004.
[53] J.S. Shin, A study of flow condensation heat transfer inside mini-channels with new experimental techniques (Ph.D. thesis), Pohang University of Science and Technology, Korea, 2004.
[54] X. Tu, P.S. Hrnjak, Flow and heat transfer in microchannels 30 to 300 microns in hydraulic diameter, Report No. ACRC CR-53, Air Conditioning and Refrigeration Center, University of Illinois at Urbana-Champaign, 2004.
[55] A. Cavallini, D.D. Col, L. Doretti, M. Matkovic, L. Rossetto, C. Zilio, Two-phase frictional pressure gradient of R236ea, R134a, and R410A inside multi-port mini-channels, Exp. Therm. Fluid Sci. 29 (2005) 861–870.

[56] I.Y. Chen, C.L. Won, C.C. Wang, Influence of oil on R-410A two-phase frictional pressure drop in a small U-type wavy tube, Int. Commun. Heat Mass Transfer 32 (2005) 797–808.
[57] B. Mitra, Supercritical gas cooling and condensation of refrigerant R410A at near-critical pressures (Ph.D. thesis), Georgia Institute of Technology, GA, 2005.
[58] U.C. Andresen, Supercritical gas cooling and near-critical-pressure condensation of refrigerant blends in microchannels (Ph.D. thesis), Georgia Institute of Technology, GA, 2006.
[59] N.J. English, S.G. Kandlikar, An experimental investigation into the effect of surfactants on air-water two-phase flow in minichannels, Heat Transfer Eng. 27 (2006) 99–109.
[60] Y.W. Hwang, M.S. Kim, The pressure drop in microtubes and the correlation development, Int. J. Heat Mass Transfer 49 (2006) 1804–1812.
[61] R. Yun, J.H. Heo, Y. Kim, Evaporative heat transfer and pressure drop of R410A in microchannels, Int. J. Refrig. 29 (2006) 92–100.
[62] B.S. Field, P.S. Hrnjak, Two-phase pressure drop and flow regime of refrigerants and refrigerant-oil mixtures in small channels, Report No. ACRC TR-261, Air Conditioning and Refrigeration Center, University of Illinois at Urbana-Champaign, 2007.
[63] C.Y. Park, P.S. Hrnjak, Carbon dioxide and R410A flow boiling heat transfer, pressure drop and flow pattern in horizontal tubes at low temperatures, Report No. ACRC TR-258, Air Conditioning and Refrigeration Center, University of Illinois at Urbana-Champaign, 2007.
[64] R. Revellin, J.R. Thome, Adiabatic two-phase frictional pressure drops in microchannels, Exp. Therm. Fluid Sci. 31 (2007) 673–685.
[65] J. Yue, G. Chen, Q. Yuan, L. Luo, Y. Gonthier, Hydrodynamics and mass transfer characteristics in gas–liquid flow through a rectangular microchannel, Chem. Eng. Sci. 62 (2007) 2096–2108.
[66] X. Quan, P. Cheng, H. Wu, An experimental investigation on pressure drop of steam condensing in silicon microchannels, Int. J. Heat Mass Transfer 51 (2008) 5454–5458.
[67] K. Dutkowski, Two-phase pressure drop of air-water in minichannels, Int. J. Heat Mass Transfer 52 (2009) 5185–5192.
[68] K.A. Marak, Condensation heat transfer and pressure drop for methane and binary methane fluids in small channels (Ph.D. thesis), Norwegian University of Science and Technology, Norway, 2009.
[69] C.Y. Park, P.S. Hrnjak, CO_2 flow condensation heat transfer and pressure drop in multi-port microchannels at low temperatures, Int. J. Refrig. 32 (2009) 1129–1139.
[70] X. Huang, G. Ding, H. Hu, Y. Zhu, Y. Gao, B. Deng, Two-phase frictional pressure drop characteristics of R410A-oil mixture flow condensation inside 4.18 mm and 1.6 mm i.d. horizontal smooth tubes, HVAC&R Res. 16 (2010) 453–470.
[71] C.W. Choi, D.I. Yu, M.H. Kim, Adiabatic two-phase flow in rectangular microchannels with different aspect ratios – Part I: Flow pattern, pressure drop and void fraction, Int. J. Heat Mass Transfer 54 (2011) 616–624.
[72] M. Ducoulombier, S. Colasson, J. Bonjour, P. Haberschill, Carbon dioxide flow boiling in a single microchannel – Part I: Pressure drops, Exp. Therm. Fluid Sci. 35 (2011) 581–596.
[73] C.B. Tibiriçá, G. Ribatski, Two-phase frictional pressure drop and flow boiling heat transfer for R245fa in a 2.32-mm tube, Heat Transfer Eng. 32 (2011) 1139–1149.
[74] A.M. Lezzi, A. Niro, G.P. Beretta, Experimental data on CHF for forced convection water boiling in long horizontal capillary tubes, in: Proc. 10th Int. Heat Transfer Conf., UK, 7, 1994, pp. 491–496.
[75] T.N. Tran, Pressure drop and heat transfer study of two-phase flow in small channels (Ph.D. thesis), Texas Tech University, TX, 1998.
[76] J. Pettersen, Flow vaporization of CO_2 in microchannel tubes (Ph.D. thesis), Norwegian University of Science and Technology, Norway, 2002.
[77] X. Huo, Experimental study of flow boiling heat transfer in small diameter tubes (Ph.D. thesis), London South Bank University, UK, 2005.
[78] J. Lee, I. Mudawar, Two-phase flow in high-heat-flux micro-channel heat sink for refrigeration cooling applications – Part I: pressure drop characteristics, Int. J. Heat Mass Transfer 48 (2005) 928–940.
[79] W. Owhaib, C. Martín-Callizo, B. Palm, Two-phase flow pressure drop of R-134A in a vertical circular mini/micro channel, in: ASME Sixth Int. Conf. on Nanochannels, Microchannels, and Minichannels, Germany, ICNMM2008-62243, 2008, pp. 343–353.
[80] H.T. Hu, G.L. Ding, X.C. Huang, B. Deng, Y.F. Gao, Pressure drop during horizontal flow boiling of R410A/oil mixture in 5 mm and 3 mm smooth tubes, Appl. Therm. Eng. 29 (2009) 3353–3365.
[81] J.M. Quibén, L. Cheng, R. Lima, J.R. Thome, Flow boiling in horizontal flattened tubes – Part I: Two-phase frictional pressure drop results and model, Int. J. Heat Mass Transfer 52 (2009) 3634–3644.
[82] M. Ducoulombier, Ebullition convective du dioxyde de carbone – étude expérimentale en micro-canal (Ph.D. thesis), Institut National des Sciences Appliquées (INSA) de Lyon, France, 2010.
[83] C.B. Tibiriçá, J.D. Silva, G. Ribatski, Experimental investigation of flow boiling pressure drop of R134A in a microscale horizontal smooth tube, J. Therm. Sci. Eng. Appl. – Trans. ASME 3 (2011) 011006.
[84] J. Wu, T. Koettig, Ch. Franke, D. Helmer, T. Eisel, F. Haug, J. Bremer, Investigation of heat transfer and pressure drop of CO_2 two-phase flow in a horizontal minichannel, Int. J. Heat Mass Transfer 54 (2011) 2154–2162.
[85] C.R. Kharangate, I. Mudawar, M.M. Hasan, Experimental and theoretical study of critical heat flux in vertical upflow with inlet vapor void, Int. J. Heat Mass Transfer 55 (2012) 360–374.
[86] M.H. Maqbool, B. Palm, R. Khodabandeh, Flow boiling of ammonia in vertical small diameter tubes: two phase frictional pressure drop results and assessment of prediction methods, Int. J. Therm. Sci. 54 (2012) 1–12.
[87] W.H. McAdams, W.K. Woods, L.C. Heroman, Vaporization inside horizontal tubes – II: Benzene–oil mixture, Trans. ASME 64 (1942) 193–200.
[88] W.W. Akers, H.A. Deans, O.K. Crosser, Condensing heat transfer within horizontal tubes, Chem. Eng. Prog. 54 (1958) 89–90.
[89] A. Cicchitti, C. Lombardi, M. Silvestri, G. Soldaini, R. Zavalluilli, Two-phase cooling experiments-pressure drop, heat transfer and burnout measurements, Energia Nucleare 7 (1960) 407–425.
[90] W.L. Owens, Two-phase pressure gradient, Int. Dev. Heat Transfer, Pt. II, ASME, New York, 1961.
[91] A.E. Dukler, M. Wicks, R.G. Cleaveland, Pressure drop and hold up in two-phase flow, AIChE J. 10 (1964) 38–51.
[92] D.R.H. Beattie, P.B. Whalley, A simple two-phase frictional pressure drop calculation method, Int. J. Multiphase Flow 8 (1982) 83–87.
[93] S. Lin, C.C.K. Kwok, R.Y. Li, Z.H. Chen, Z.Y. Chen, Local frictional pressure drop during vaporization of R-12 through capillary tubes, Int. J. Multiphase Flow 17 (1991) 95–102.
[94] R.W. Lockhart, R.C. Martinelli, Proposed correlation of data for isothermal two-phase, two-component flow in pipes, Chem. Eng. Prog. 45 (1949) 39–48.
[95] L. Friedel, Improved friction pressure drop correlations for horizontal and vertical two-phase pipe flow, European Two-Phase Group Meeting, Ispra, Italy, 1979, Paper E2.
[96] H. Müller-Steinhagen, K. Heck, A simple friction pressure drop correlation for two-phase flow in pipes, Chem. Eng. Process. 20 (1986) 297–308.
[97] D.S. Jung, R. Radermacher, Prediction of pressure drop during horizontal annular flow boiling of pure and mixed refrigerants, Int. J. Heat Mass Transfer 32 (1989) 2435–2446.
[98] C.C. Wang, C.S. Chiang, D.C. Lu, Visual observation of two-phase flow pattern of R-22, R-134a, and R-407C in a 6.5-mm smooth tube, Exp. Therm. Fluid Sci. 15 (1997) 395–405.
[99] K. Mishima, T. Hibiki, Some characteristics of air–water two-phase flow in small diameter vertical tubes, Int. J. Multiphase Flow 22 (1996) 703–712.
[100] Y.Y. Yan, T.F. Lin, Evaporation heat transfer and pressure drop of refrigerant R-134a in a small pipe, Int. J. Heat Mass Transfer 41 (1998) 4183–4194.
[101] Y.Y. Yan, T.F. Lin, Condensation heat transfer and pressure drop of refrigerant R-134a in a small pipe, Int. J. Heat Mass Transfer 42 (1999) 697–708.
[102] T.N. Tran, M.C. Chyu, M.W. Wambsganss, D.M. France, Two-phase pressure drop of refrigerants during flow boiling in small channels: an experimental investigation and correlation development, Int. J. Multiphase Flow 26 (2000) 1739–1754.
[103] I.Y. Chen, K.S. Yang, Y.J. Chang, C.C. Wang, Two-phase pressure drop of air-water and R-410A in small horizontal tubes, Int. J. Multiphase Flow 27 (2001) 1293–1299.
[104] H.J. Lee, S.Y. Lee, Pressure drop correlations for two-phase flow within horizontal rectangular channels with small heights, Int. J. Multiphase Flow 27 (2001) 783–796.
[105] W. Yu, D.M. France, M.W. Wambsganss, J.R. Hull, Two-phase pressure drop, boiling heat transfer, and critical heat flux to water in a small-diameter horizontal tube, Int. J. Multiphase Flow 28 (2002) 927–941.
[106] L. Sun, K. Mishima, Evaluation analysis of prediction methods for two-phase flow pressure drop in mini-channels, Int. J. Multiphase Flow 35 (2009) 47–54.
[107] W. Li, Z. Wu, A general correlation for adiabatic two-phase pressure drop in micro/mini-channels, Int. J. Heat Mass Transfer 53 (2010) 2732–2739.
[108] W. Zhang, T. Hibiki, K. Mishima, Correlations of two-phase frictional pressure drop and void fraction in mini-channel, Int. J. Heat Mass Transfer 53 (2010) 453–465.
[109] W. Li, Z. Wu, Generalized adiabatic pressure drop correlations in evaporative micro/mini-channels, Exp. Therm. Fluid Sci. 35 (2011) 866–872.
[110] M.B. Bowers, I. Mudawar, Two-phase electronic cooling using mini-channel and micro-channel heat sinks – Part 2: Flow rate and pressure drop constraints, J. Electron. Packag. – Trans. ASME 116 (1994) 298–305.
[111] A.E. Bergles, Review of instability in two-phase systems, in: S. Kakac, F. Mayinger (Eds.), Two-Phase Flows and Heat Transfer, vol. 1, Hemisphere, Washington, DC, 1977, pp. 383–422.
[112] G. Yadigaroglu, Two-phase flow instabilities and propagation phenomena, in: J.M. Delhaye, M. Giot, M.L. Riethmuller (Eds.), Thermohydraulics of Two-Phase Systems for Industrial Design and Nuclear Engineering, Hemisphere, Washington, DC, 1981, pp. 353–403.
[113] S.M. Zivi, Estimation of steady-state steam void-fraction by means of the principle of minimum entropy production, J. Heat Transfer – Trans. ASME 86 (1964) 247–252.
[114] F.P. Incropera, D.P. Dewitt, Fundamentals of Heat and Mass Transfer, fifth ed., Wiley, New York, 2002.
[115] R.K. Shah, A.L. London, Laminar Flow Forced Convection in Ducts: A Source Book for Compact Heat Exchanger Analytical Data, Suppl. 1, Academic press, New York, 1978.
[116] S.M. Kim, I. Mudawar, Universal approach to predicting two-phase frictional pressure drop for adiabatic and condensing mini/micro-channel flows, Int. J. Heat Mass Transfer 55 (2012) 3246–3261.

[117] S.M. Kim, I. Mudawar, Universal approach to predicting two-phase frictional pressure drop for mini/micro-channel saturated flow boiling, Int. J. Heat Mass Transfer 58 (2013) 718–734.
[118] S.M. Kim, I. Mudawar, Universal approach to predicting heat transfer coefficient for condensing mini/micro-channel flows, Int. J. Heat Mass Transfer 56 (2013) 238–250.
[119] S.M. Kim, I. Mudawar, Universal approach to predicting saturated flow boiling heat transfer in mini/micro-channels – Part II: Two-phase heat transfer coefficient, Int. J. Heat Mass Transfer 64 (2013) 1239–1256.
[120] S.M. Kim, I. Mudawar, Universal approach to predicting saturated flow boiling heat transfer in mini/micro-channels – Part I: Dryout incipience quality, Int. J. Heat Mass Transfer 64 (2013) 1226–1238.
[121] D.D. Hall, I. Mudawar, Critical heat flux (CHF) for water flow in tubes – I: Compilation and assessment of world CHF data, Int. J. Heat Mass Transfer 43 (2000) 2573–2604.
[122] D.D. Hall, I. Mudawar, Critical heat flux (CHF) for water flow in tubes – II: Subcooled CHF correlations, Int. J. Heat Mass Transfer 43 (2000) 2605–2640.
[123] C.J. Baroczy, Correlation of liquid fraction in two-phase flow with applications to liquid metals, Chem. Eng. Prog. 61 (1965) 179–191.
[124] S.Z. Rouhani, E. Axelsson, Calculation of void volume fraction in the subcooled and quality boiling region, Int. J. Heat Mass Transfer 13 (1970) 393.
[125] E.W. Lemmon, M.L. Huber, M.O. McLinden, Reference fluid thermodynamic and transport properties, REFPROP Version 8.0, NIST, MD, 2007.
[126] M.A. Woldesemayat, A.J. Ghajar, Comparison of void fraction correlations for different flow patterns in horizontal and upward inclined pipes, Int. J. Multiphase Flow 33 (2007) 347–370.
[127] H.M. Soliman, The mist-annular transition during condensation and its influence on the heat transfer mechanism, Int. J. Multiphase Flow 12 (1986) 277–288.
[128] E.S. AL-Hajri, Prediction of heat transfer and pressure drop of condensing refrigerant flow in a high aspect ratio micro-channels (Ph.D. thesis), University of Maryland, College Park, MD, 2009.
[129] A. Megahed, I. Hassan, Two-phase pressure drop and flow visualization of FC-72 in a silicon microchannel heat sink, Int. J. Heat Fluid Flow 30 (2009) 1171–1182.
[130] R. Revellin, Experimental two-phase fluid flow in microchannels (Ph.D. thesis), École Polytechnique Fédérale de Lausanne, France, 2006.
[131] L. Chen, Y.S. Tian, T.G. Karayiannis, The effect of tube diameter on vertical two-phase flow regimes in small tubes, Int. J. Heat Mass Transfer 49 (2006) 4220–4230.
[132] T.G. Karayiannis, M.M. Mahmoud, D.B.R. Kenning, A study of discrepancies in flow boiling results in small to microdiameter metallic tubes, Exp. Therm. Fluid Sci. 36 (2012) 126–142.
[133] W. Qu, I. Mudawar, S.-Y. Lee, S.T. Wereley, Experimental and computational investigation of flow development and pressure drop in a rectangular micro-channel, J. Electron. Packag. – Trans. ASME 128 (2006) 1–9.
[134] J.E. Koskie, I. Mudawar, W.G. Tiederman, Parallel-wire probes for measurement of thick liquid films, Int. J. Multiphase Flow 15 (1989) 521–530.
[135] I. Mudawar, R.A. Houpt, Measurement of mass and momentum transport in wavy-laminar falling liquid films, Int. J. Heat Mass Transfer 36 (1993) 4151–4162.